



Image credit: ESO

Multi-frequency
linear and circular
radio polarization monitoring
of jet emission elements in Fermi blazars

Ioannis Myserlis

PhD Advisor: Dr. E. Angelakis

Collaborators:
Dr. L. Fuhrmann, Prof. V. Pavlidou
Dr. A. Kraus, V. Karamanavis, Prof. A. Zensus

Max-Planck Institut für Radioastronomie

Outline

- Polarization production mechanisms in AGN
- Polarization as a probe of micro-physics in blazars
- Polarization in the time and frequency domains

Why?

- The F-GAMMA program
- Mueller matrix analysis
- Data reduction progress

How?

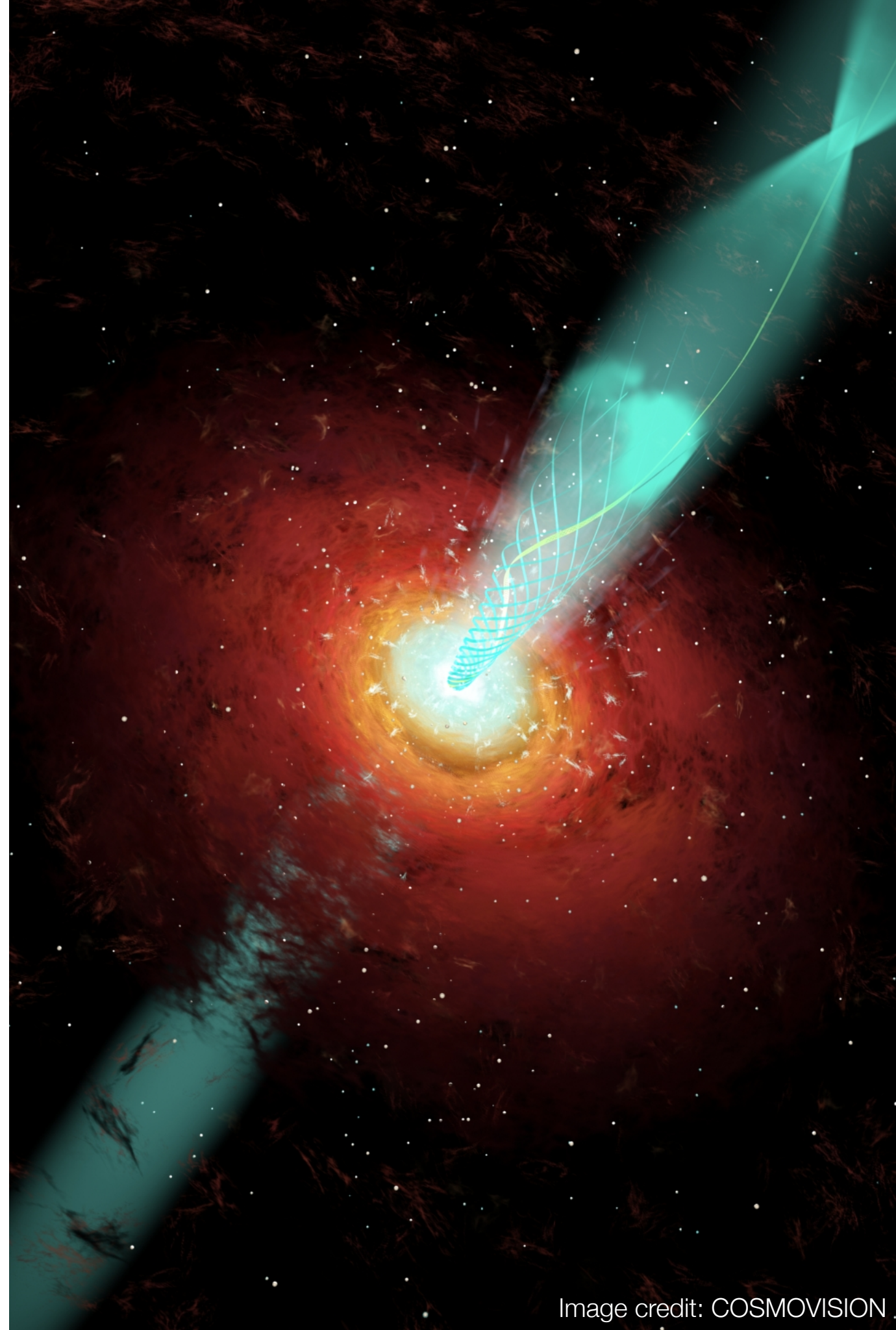
- Results

Polarization production mechanisms in AGN

Radio emission mechanism:
Incoherent synchrotron radiation

Synchrotron radiation is highly polarized

Radiative transfer effects can alter the
polarization characteristics



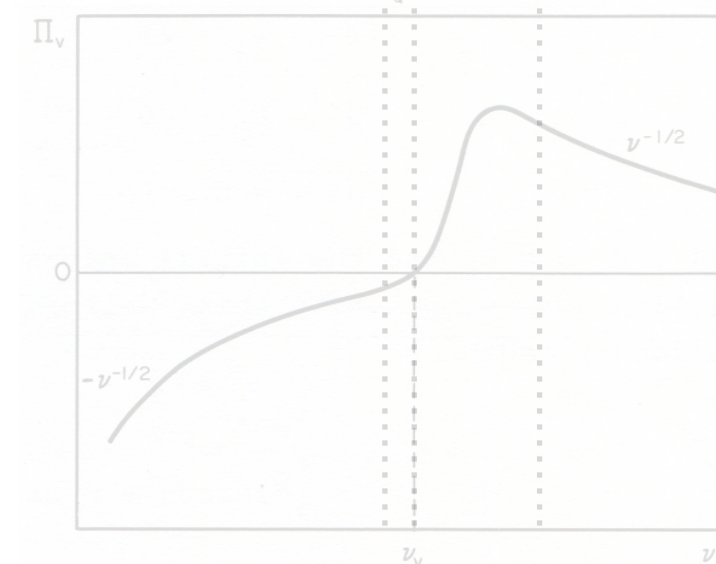
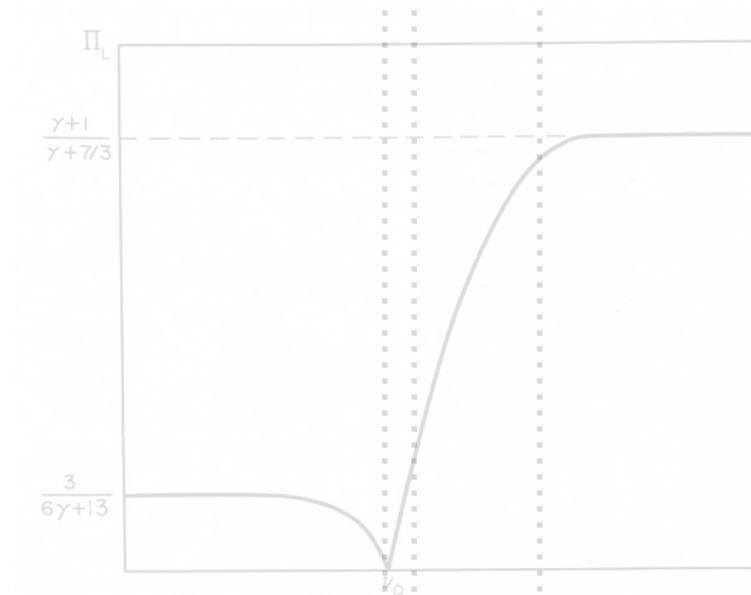
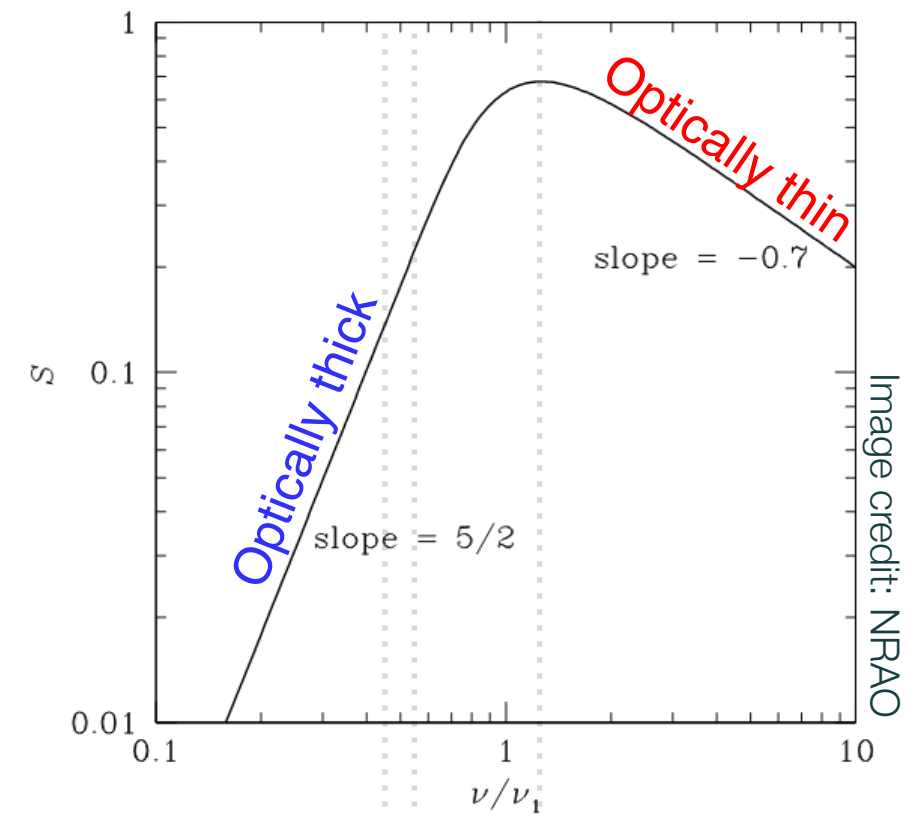
Polarization production mechanisms in AGN

Synchrotron Self Absorbed (SSA) spectrum

$$N(E)dE = \kappa E^{-s} dE \rightarrow \underline{S_\nu \propto \nu^{-\frac{s-1}{2}} = \nu^{-a}}$$

Canonical value for AGN: $a \approx 0.7$

Self absorbed $S_\nu \propto \nu^{+2.5}$



Polarization production mechanisms in AGN

Linear polarization (LP) component of synchrotron sources

- Optically thin

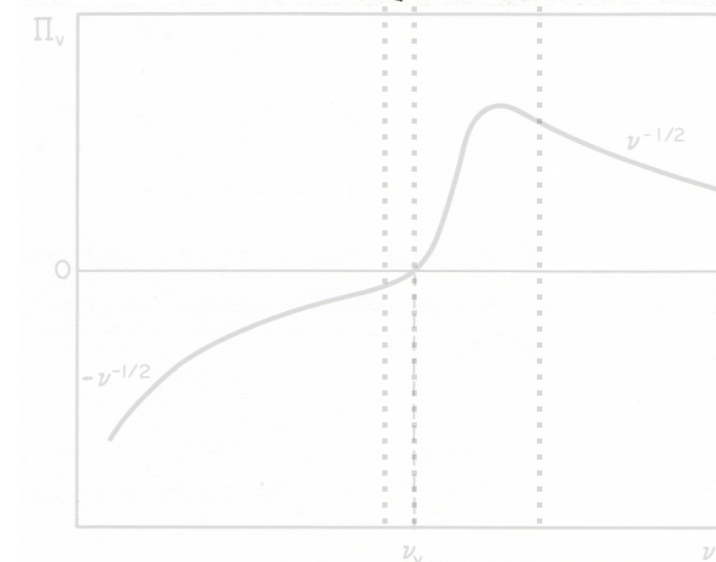
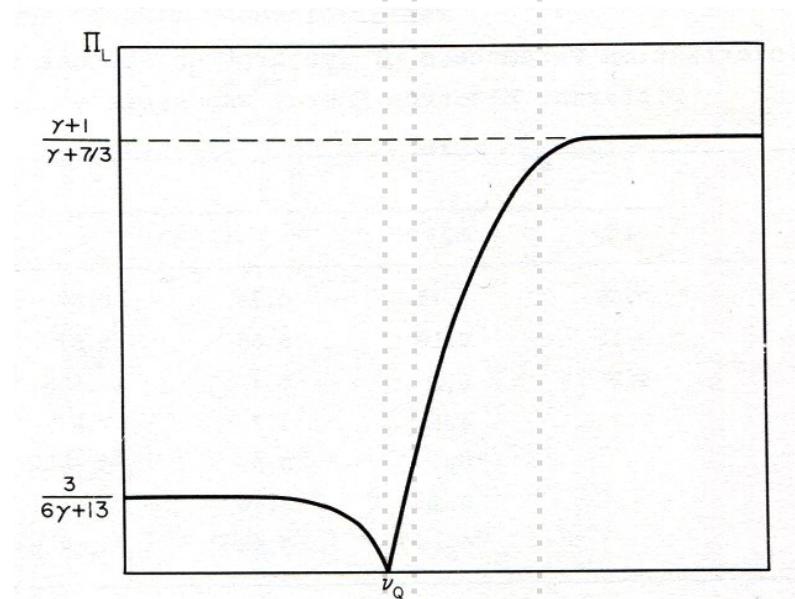
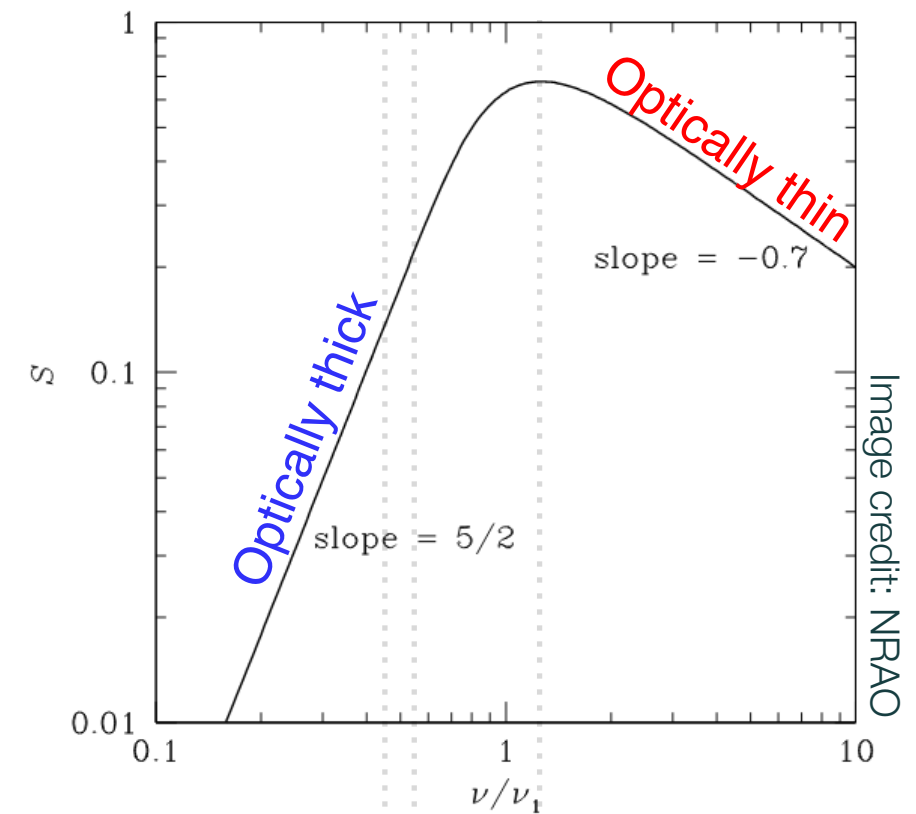
$$m_l = \frac{s+1}{s+\frac{7}{3}} = \frac{a+1}{a+\frac{5}{3}} \approx 72\%$$

Perpendicular to the projected magnetic field

- Optically thick

$$m_l = \frac{3}{6s+13} = \frac{3}{12a+19} \approx 11\%$$

Parallel to the projected magnetic field



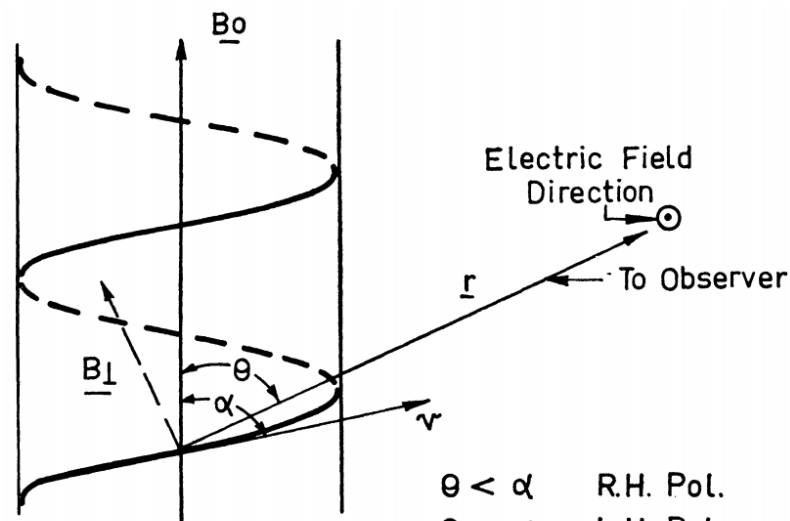
Polarization production mechanisms in AGN

Circular polarization (CP) component of synchrotron sources

Low values of circular polarization $m_c \sim 100 \left(\frac{\nu_L}{\nu} \right)^{\frac{1}{2}}$
(Sciama & Rees, 1967)

Isotropic pitch angle distribution

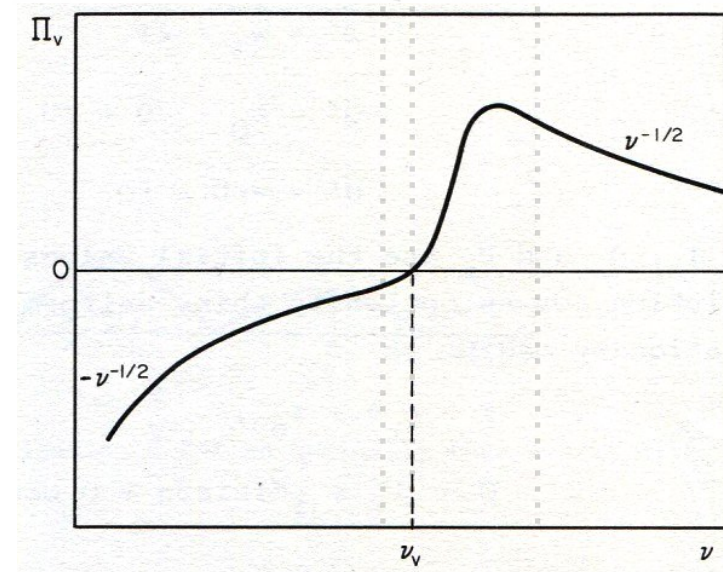
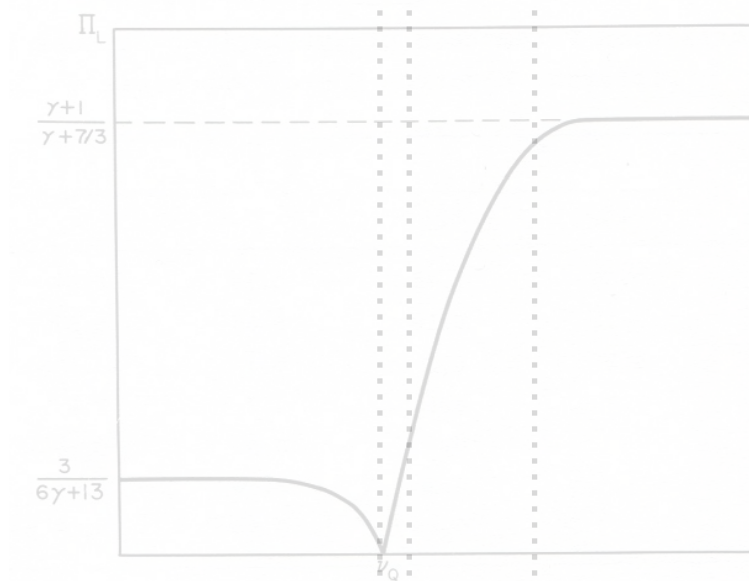
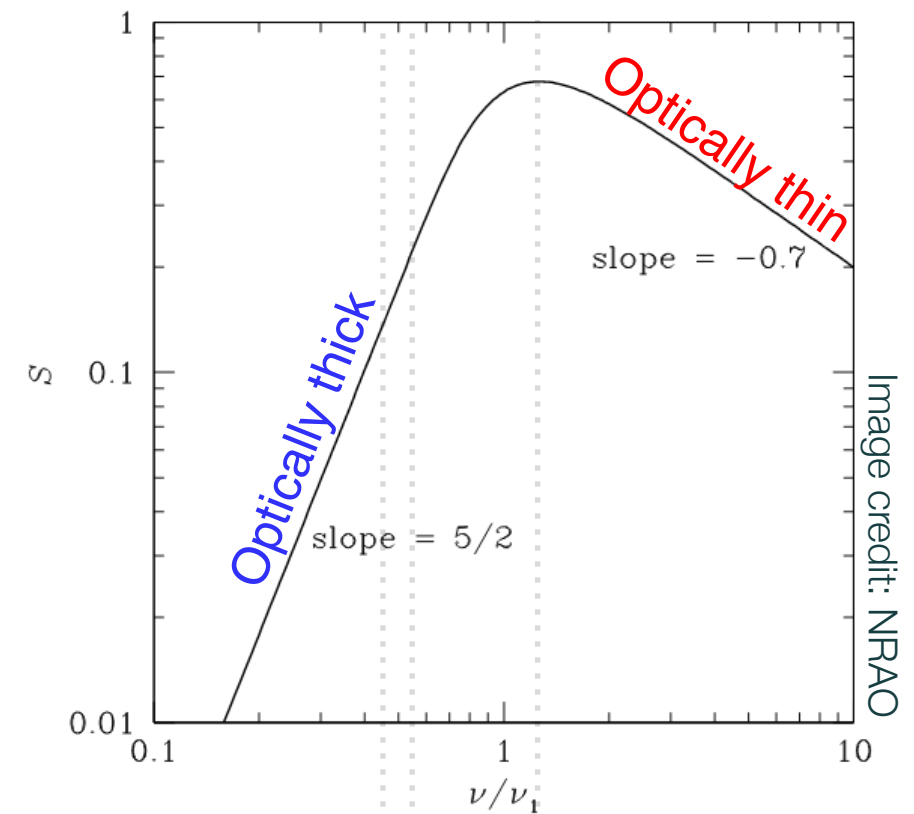
- Optically thin $m_c \propto \nu^{-\frac{1}{2}}$
- Optically thick $m_c \propto -\nu^{-\frac{1}{2}}$



Gardner & Whiteoak (1966)

$\theta < \alpha$ R.H. Pol.
 $\theta > \alpha$ L.H. Pol.

Pacholczyk A.G. (1977)



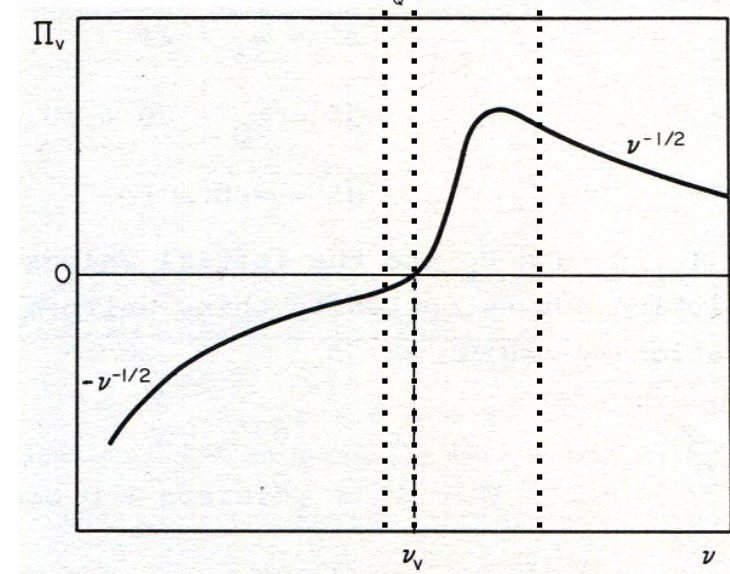
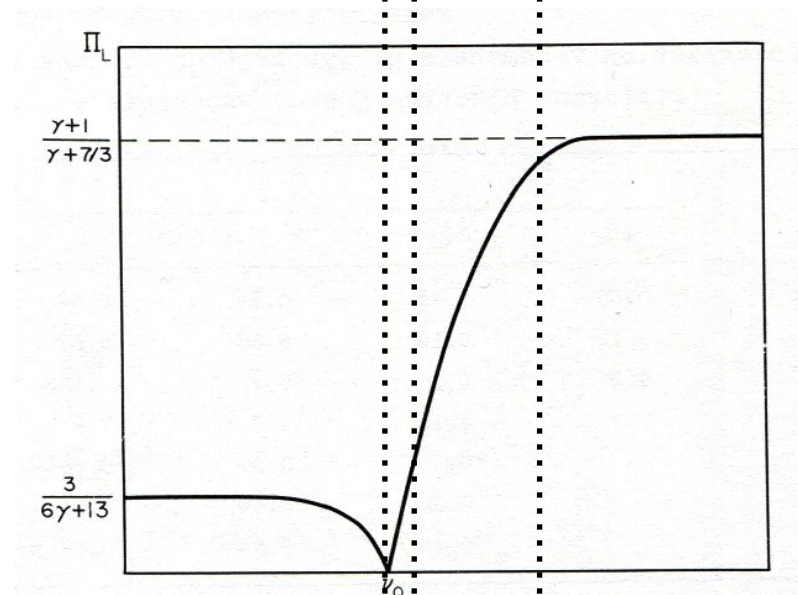
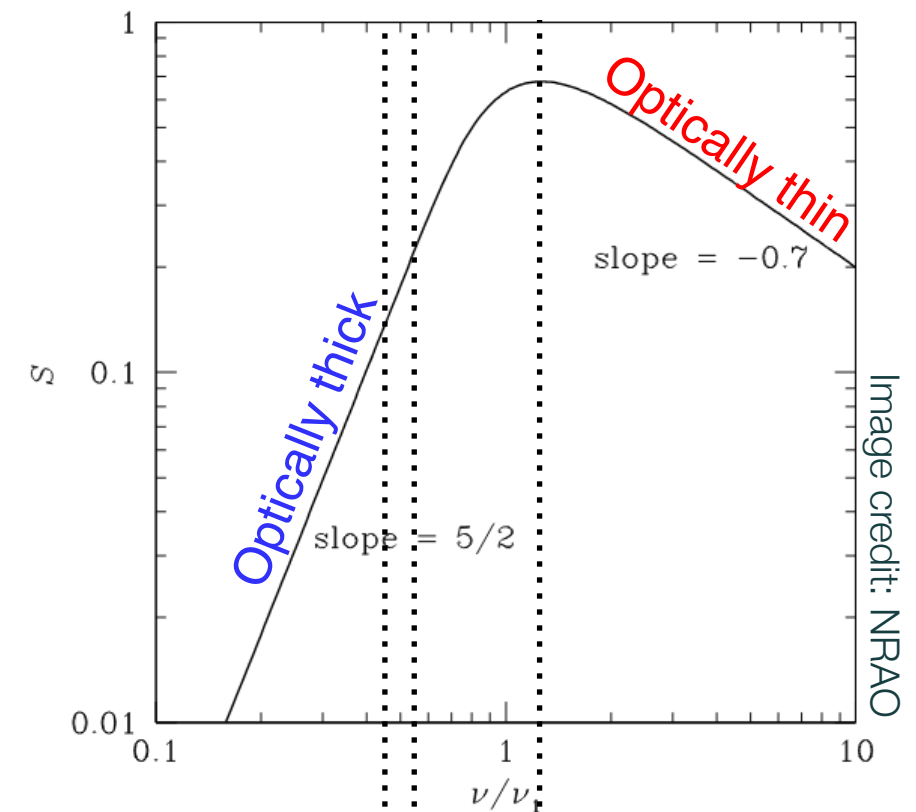
Polarization production mechanisms in AGN

Analytic description in the frequency domain

Both LP and CP decrease to 0% close to $\nu_m \rightarrow \tau = 1$

LP: $\nu_Q \approx 0.44\nu_m \rightarrow \tau \approx 7$

CP: $\nu_V \approx 0.49\nu_m \rightarrow \tau \approx 5$



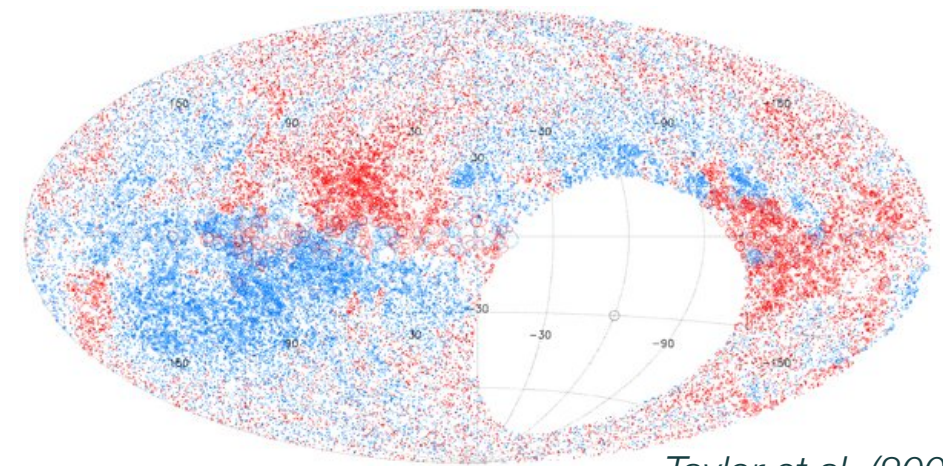
Polarization production mechanisms in AGN

Radiative transfer effects when propagating through magneto-ionic materials

Faraday rotation

LCP and RCP modes with different phase velocities

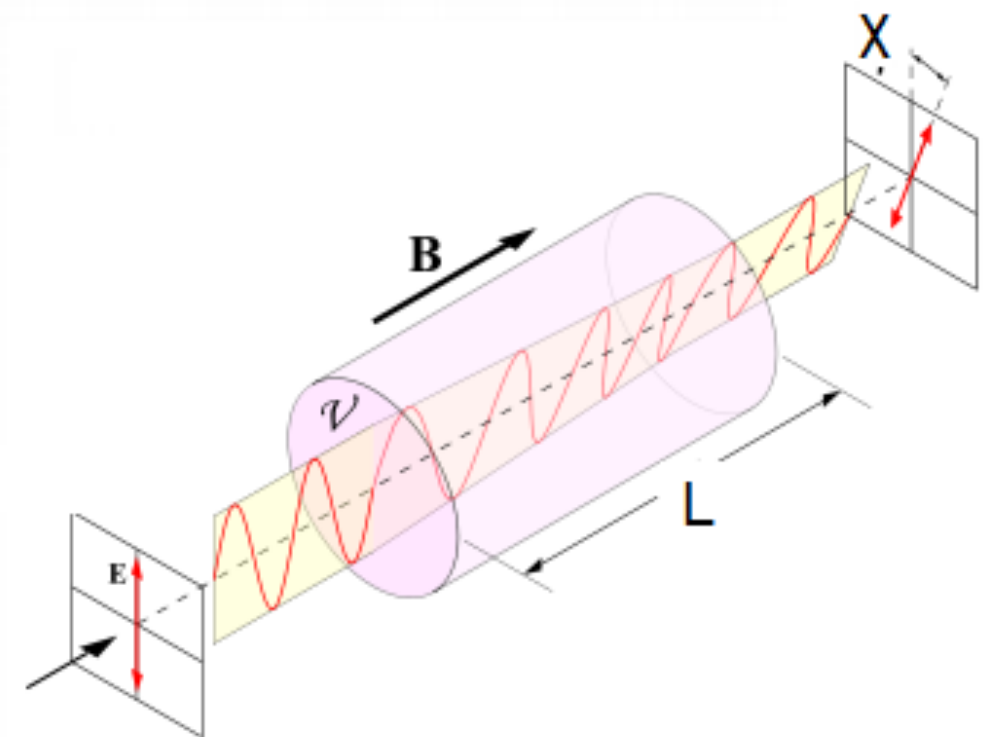
$$\Delta\chi = 8.1 \cdot 10^5 \cdot \left(\int_L n_e B_{\parallel} \cos \theta dL \right) \cdot \lambda^2 = RM \cdot \lambda^2 \quad [rad]$$



Taylor et al. (2009)

Faraday depolarization

Rotation decreases as γ increases $\propto \ln\left(\frac{\gamma}{\gamma^2}\right)$
(*Trubnikov, 1958 & Melrose, 1997a*)



Polarization production mechanisms in AGN

Radiative transfer effects when propagating through magneto-ionic materials

Faraday interconversion / pulsation

Linear \longleftrightarrow Circular polarization

Birefringence of the two orthogonal LP modes: \perp & \parallel to the magnetic field

$\propto \lambda^3$

Relativistic electrons

Polarization as a probe of micro-physics in blazars

Synchrotron polarization

Linear polarization is a measure of

B-field topology

B-field uniformity $\epsilon = \frac{B_0}{B}$

Circular polarization is a measure of

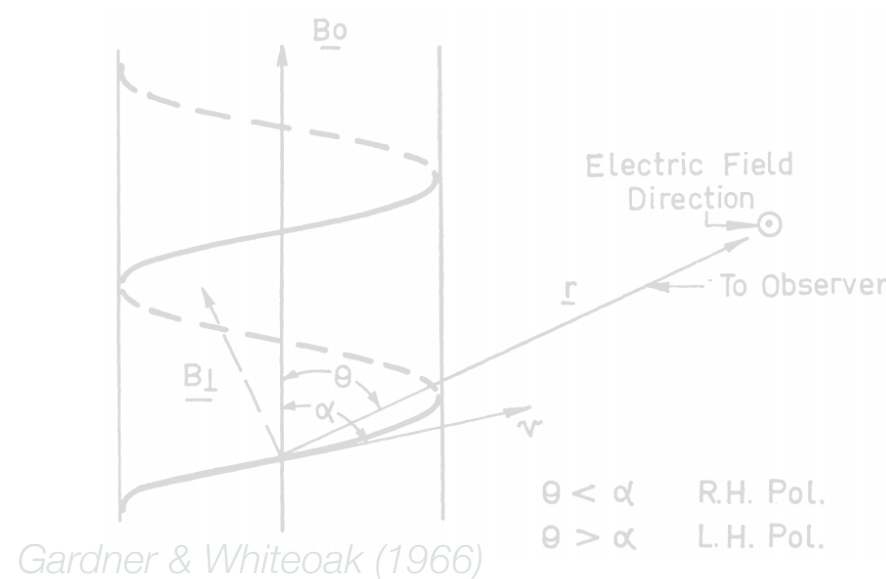
B-field magnitude

B-field uniformity

Pitch angle distribution

$$m_c \sim 100 \left(\frac{\nu_L}{\nu} \right)^{\frac{1}{2}}$$

$$p_c = - \frac{4(\gamma + 1)(\gamma + 2)}{3\gamma(\gamma + \frac{7}{3})} \frac{\Gamma\left(\frac{3\gamma + 4}{12}\right)\Gamma\left(\frac{3\gamma + 8}{12}\right)}{\Gamma\left(\frac{3\gamma - 1}{12}\right)\Gamma\left(\frac{3\gamma + 7}{12}\right)} \times \left(\text{ctg } \varphi + \frac{1}{\gamma + 2} \frac{1}{Y} \frac{dY}{d\varphi} \right) \left(\frac{B \sin \varphi}{B_v} \right)$$



Gardner & Whiteoak (1966)

Pacholczyk A.G. (1977)

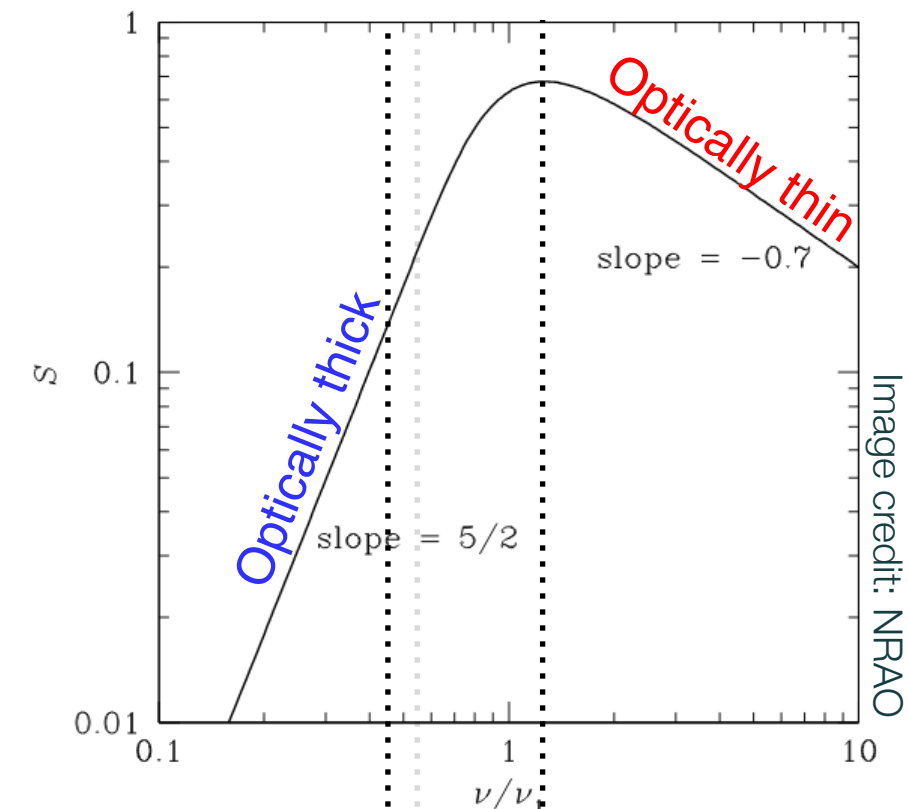
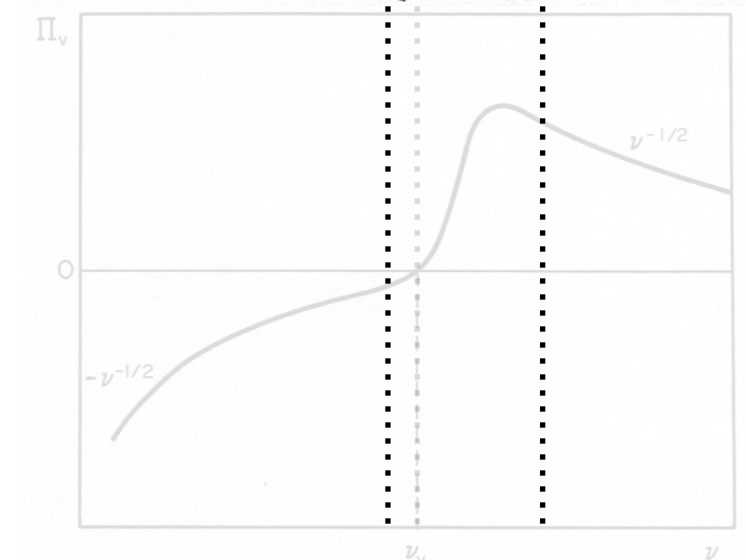
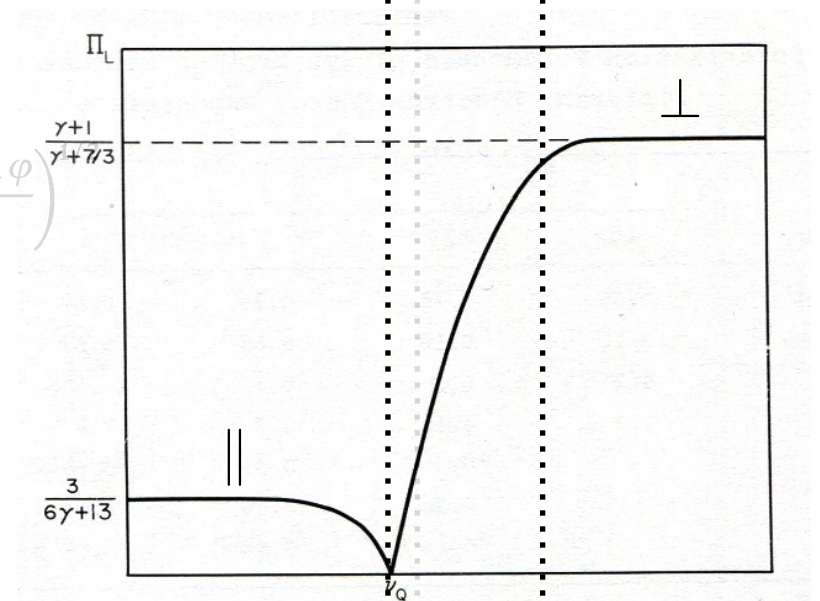


Image credit: NRAO



Polarization as a probe of micro-physics in blazars

Synchrotron polarization

Linear polarization is a measure of

B-field topology

B-field uniformity $\epsilon = \frac{B_0}{B}$

Circular polarization is a measure of

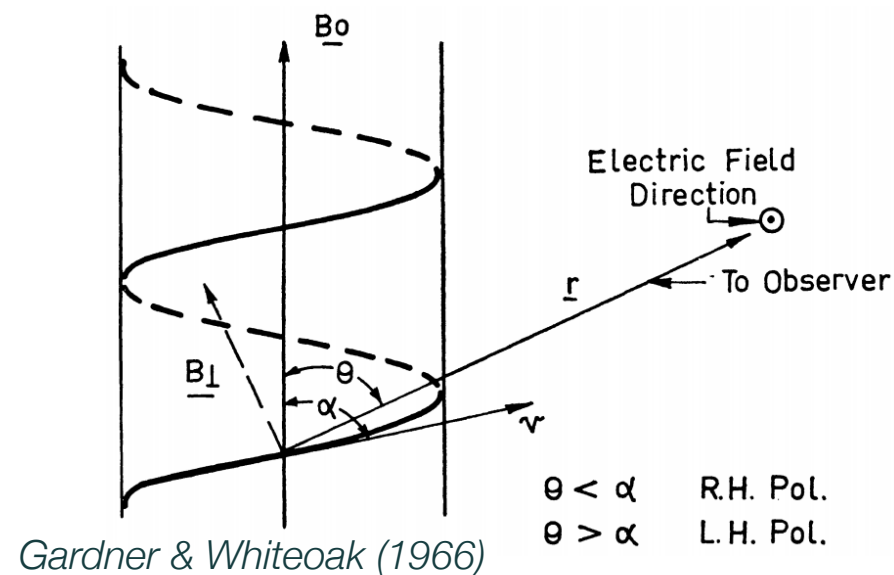
B-field magnitude

B-field uniformity

Pitch angle distribution

$$m_c \sim 100 \left(\frac{\nu_L}{\nu} \right)^{\frac{1}{2}}$$

$$p_c = - \frac{4(\gamma + 1)(\gamma + 2)}{3\gamma(\gamma + \frac{7}{3})} \frac{\Gamma\left(\frac{3\gamma + 4}{12}\right)\Gamma\left(\frac{3\gamma + 8}{12}\right)}{\Gamma\left(\frac{3\gamma - 1}{12}\right)\Gamma\left(\frac{3\gamma + 7}{12}\right)} \times \left(\text{ctg } \varphi + \frac{1}{\gamma + 2} \frac{1}{Y} \frac{dY}{d\varphi} \right) \left(\frac{B \sin \varphi}{B_\nu} \right)$$



Gardner & Whiteoak (1966)

Pacholczyk A.G. (1977)

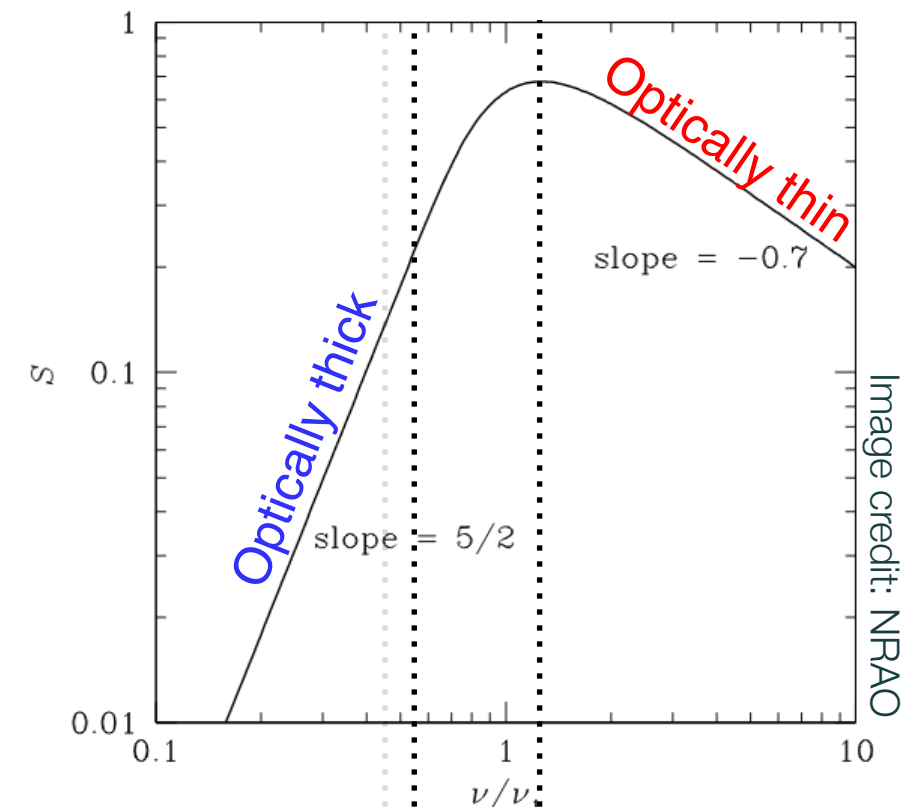
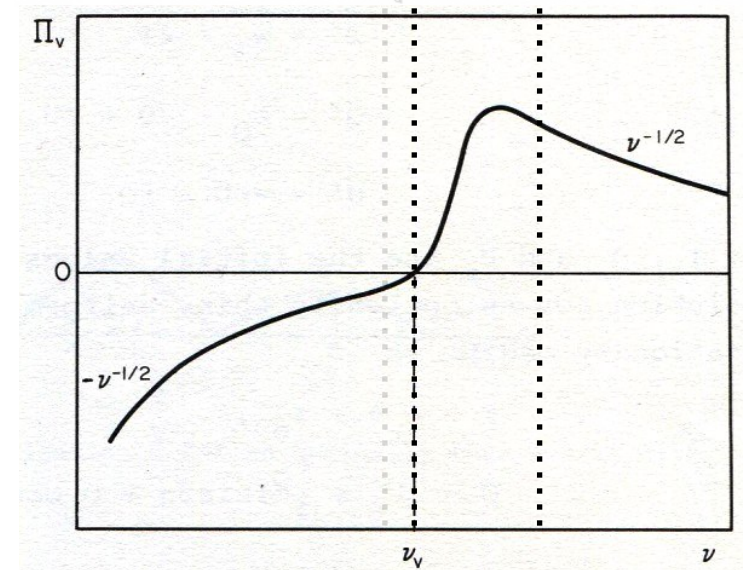
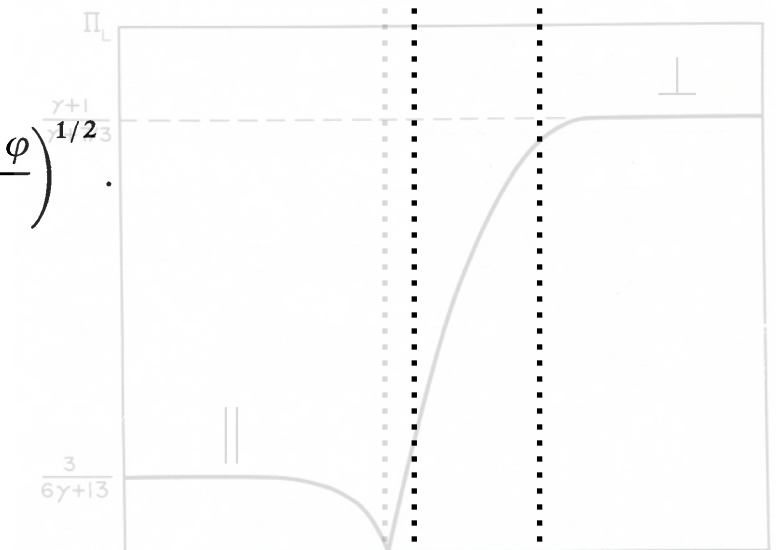


Image credit: NRAO



Polarization as a probe of micro-physics in blazars

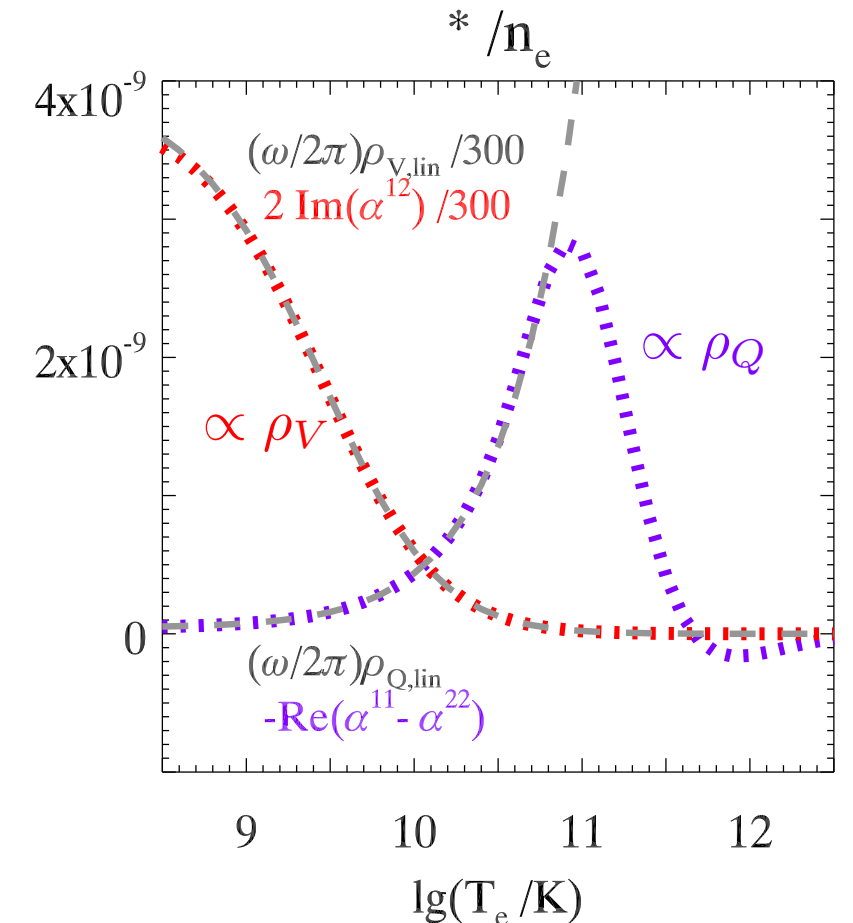
Radiative transfer coefficients through the jet plasma

Faraday rotation (FR) and conversion (FC) coefficients

Diversity between different plasma states, e.g. cold or relativistic

LP/CP degrees ratio is a measure of the FR/FC coefficients ratio

Investigate the state of the jet plasma



Huang & Shcherbakov (2011)

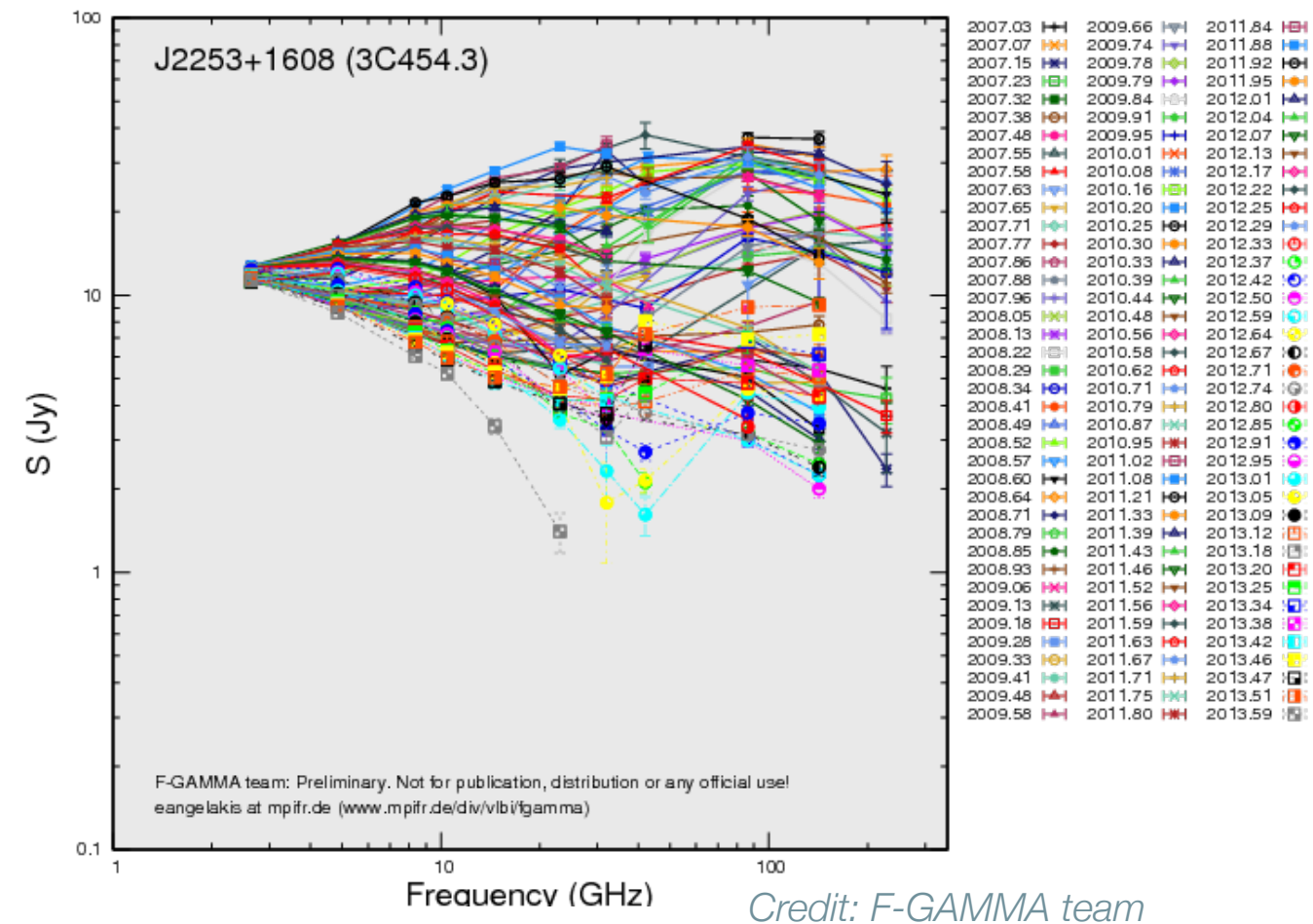
$$\frac{d\mathbf{S}}{ds} = \begin{pmatrix} \varepsilon_I \\ \varepsilon_Q \\ 0 \\ \varepsilon_V \end{pmatrix} - \begin{pmatrix} \eta_I & \eta_Q & 0 & \eta_V \\ \eta_Q & \eta_I & \rho_V & 0 \\ 0 & -\rho_V & \eta_I & \rho_Q \\ \eta_V & 0 & -\rho_Q & \eta_I \end{pmatrix} \mathbf{S}$$

Polarization in the time and frequency domains

Synchrotron polarization characteristics have an analytical description in the frequency domain

Blazar variability:
Propagation of high energy SED synchrotron components through the observed bandpass
(*Marscher & Gear 1985*)

Multi-band monitoring to trace the evolution of the physical characteristics



Polarization in the time and frequency domains

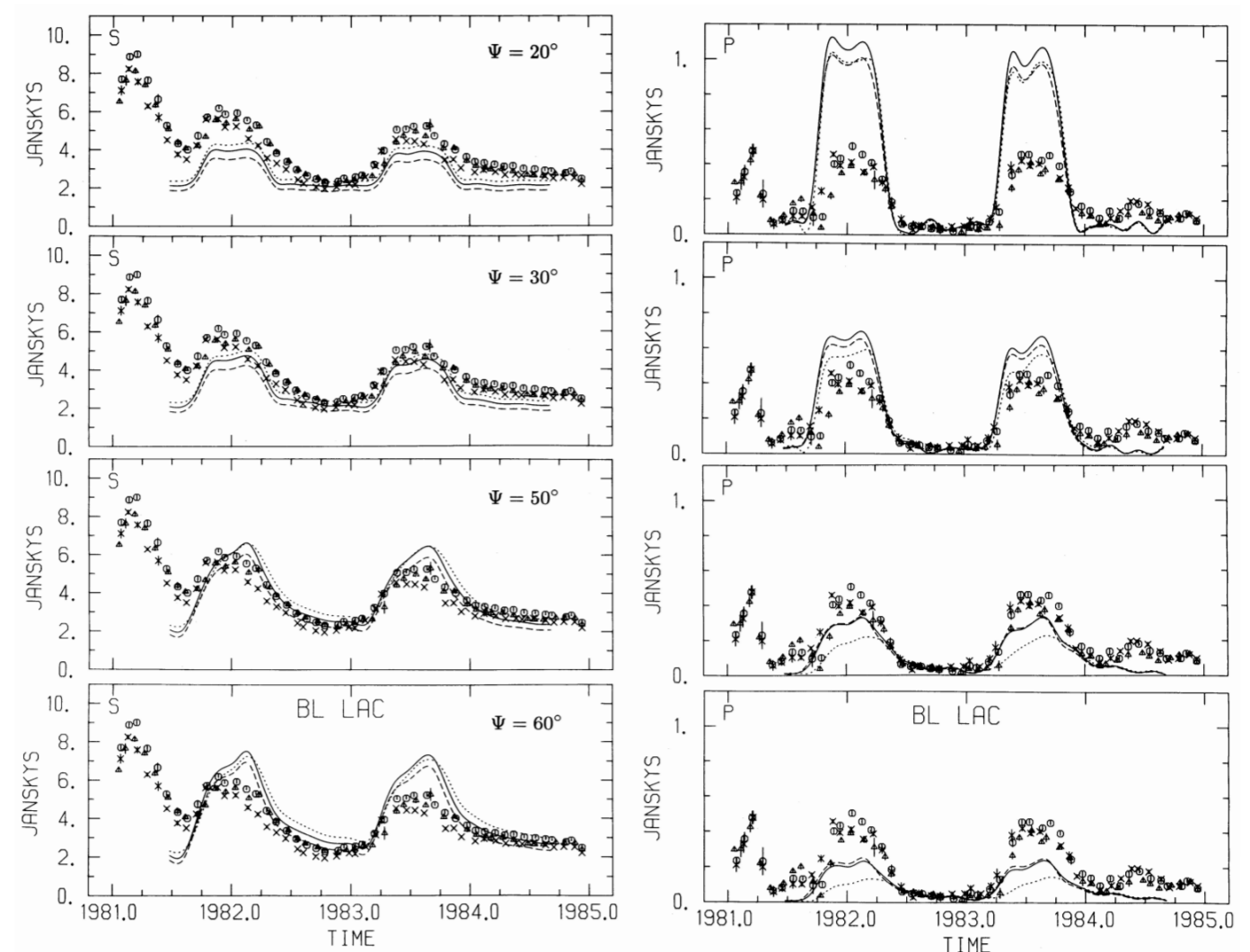
Testing variability models (e.g. shock-in-jet model)

Multi-frequency polarization monitoring

Rotation measure studies

Multi-band polarization monitoring

Connection between different jet emitting regions



Polarization in the time and frequency domains

Polarization Rotator Events (angle swings)

Geometrical swing

Emission element on helical path

Arbitrary magnitude

Radiative "swing"

Emission element expansion

Optical depth evolution

LP drops to 0% and gets to optically thin/thick values

CP drops to 0% and changes handedness

Exactly 90 degrees

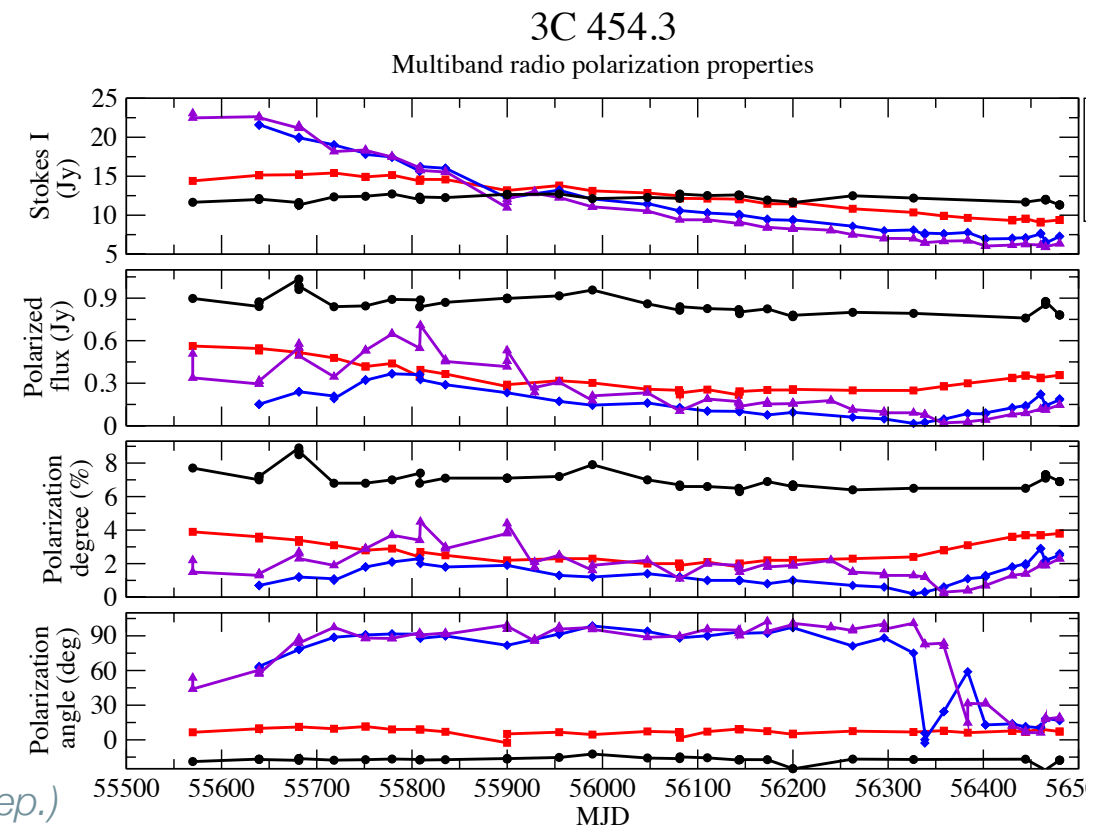
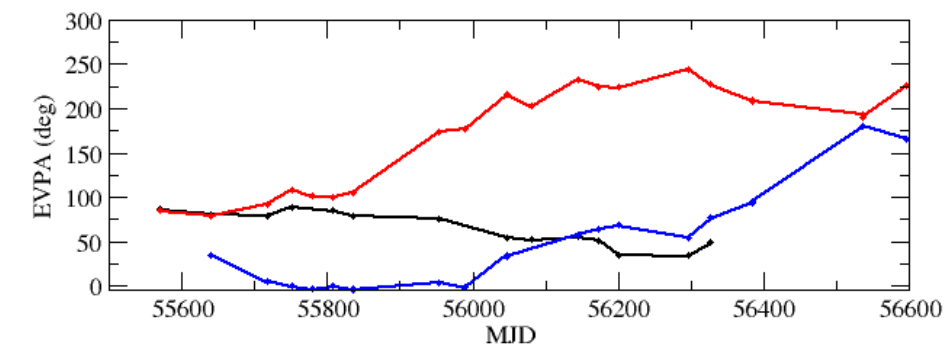
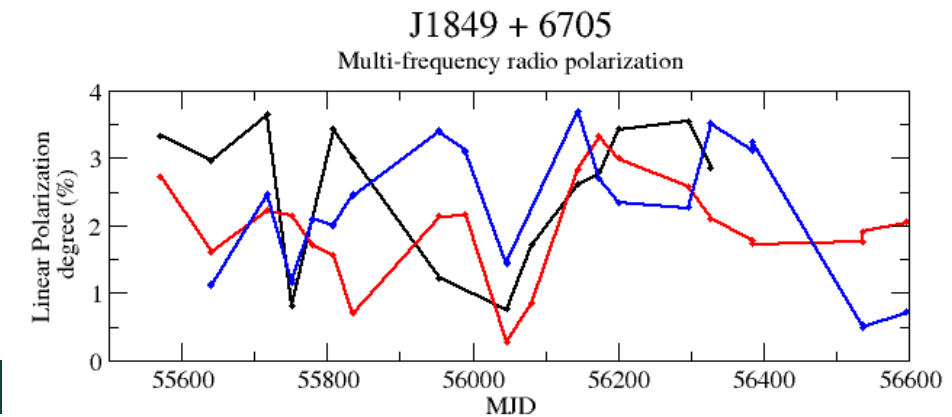
The mechanisms can operate simultaneously

Radiative "swings" can only be studied

at low radio frequencies

Geometrical

Radiative



The F-GAMMA program

Multifrequency monthly monitoring of 60 γ -ray blazars

Flux density variability

Spectral evolution

Polarization variability

Main facilities

100m Effelsberg telescope (Germany)

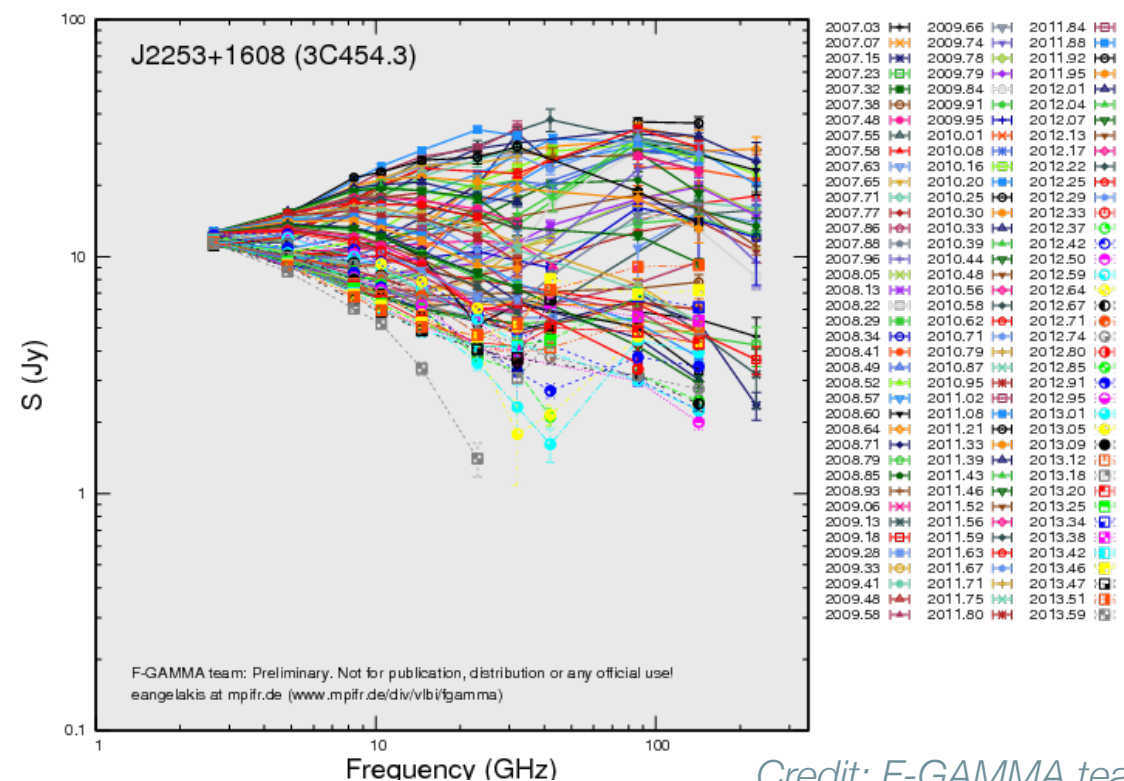
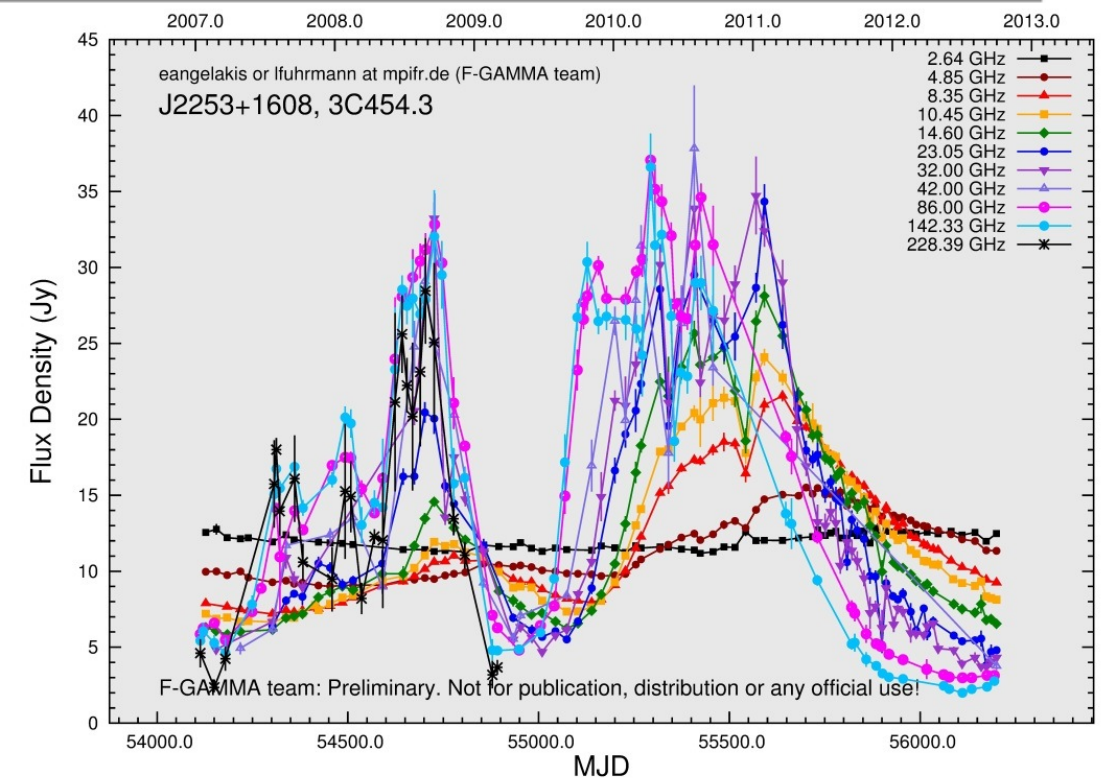
2.64, 4.85, 8.35, 10.45, 14.60, 23.05, 32.00, 42.90 GHz

30m Pico Veleta IRAM (Spain)

88.24, 142.33, 228.39 GHz

12m APEX

345 GHz



The F-GAMMA program

4.85 GHz

LP: 75% of the sample ($\tilde{m}_l = 3.1\%$)

CP: 2% of the sample ($\tilde{m}_c = 0.4\%$)

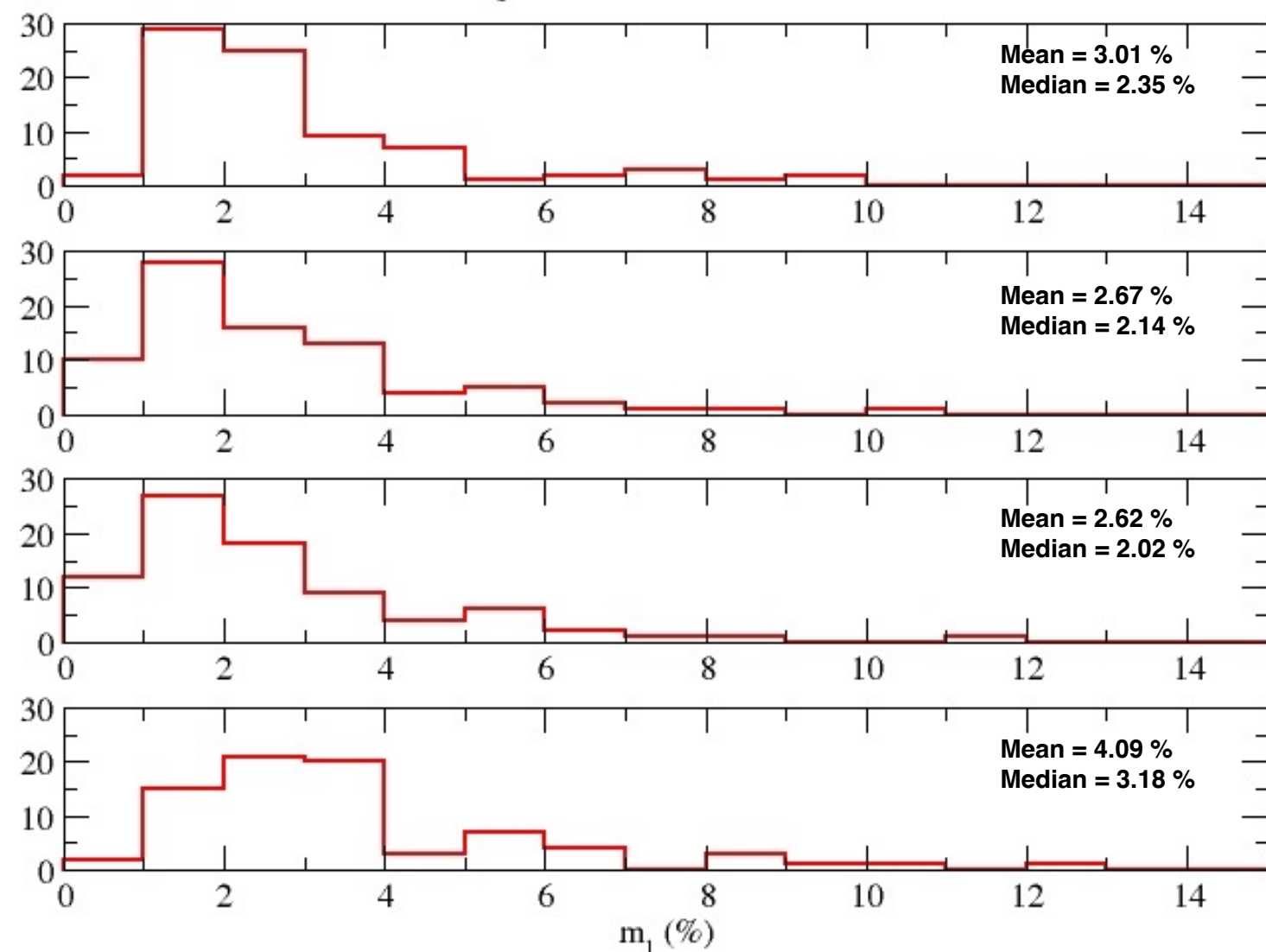
10.45 GHz

LP: 39% of the sample ($\tilde{m}_l = 3.6\%$)

CP: 5% of the sample ($\tilde{m}_c = 0.4\%$)

Mean linear polarization histograms

From top: 2.64 - 4.85 - 8.35 - 10.45 GHz



Mueller matrix analysis

$$\begin{pmatrix} I_{obs} \\ Q_{obs} \\ U_{obs} \\ V_{obs} \end{pmatrix} = \begin{pmatrix} m_{11} & m_{12} & m_{13} & m_{14} \\ m_{21} & m_{22} & m_{23} & m_{24} \\ m_{31} & m_{32} & m_{33} & m_{34} \\ m_{41} & m_{42} & m_{43} & m_{44} \end{pmatrix} \cdot \begin{pmatrix} I_{real} \\ Q_{real} \\ U_{real} \\ V_{real} \end{pmatrix}$$

$$\begin{aligned} I_{obs} &= m_{11} \cdot I_{real} + m_{12} \cdot Q_{real} + m_{13} \cdot U_{real} + m_{14} \cdot V_{real} \\ Q_{obs} &= m_{21} \cdot I_{real} + m_{22} \cdot Q_{real} + m_{23} \cdot U_{real} + m_{24} \cdot V_{real} \\ U_{obs} &= m_{31} \cdot I_{real} + m_{32} \cdot Q_{real} + m_{33} \cdot U_{real} + m_{34} \cdot V_{real} \\ V_{obs} &= m_{41} \cdot I_{real} + m_{42} \cdot Q_{real} + m_{43} \cdot U_{real} + m_{44} \cdot V_{real} \end{aligned}$$

Method

1. Observe sources with known polarization characteristics
2. Solve the system of equations [1] by fitting our measurements
3. Apply the instrumental polarization correction to our target sources

Full Stokes calibration problems

Lack of CP calibrators

Circularly polarized feeds

$$\begin{aligned} I &= |E_l|^2 + |E_r|^2, \\ Q &= 2\text{Re}(E_l^* E_r), \\ U &= -2\text{Im}(E_l^* E_r), \\ V &= |E_l|^2 - |E_r|^2. \end{aligned}$$

Mueller matrix analysis

$$\begin{pmatrix} I_{obs} \\ Q_{obs} \\ U_{obs} \\ V_{obs} \end{pmatrix} = \begin{pmatrix} m_{11} & m_{12} & m_{13} & m_{14} \\ m_{21} & m_{22} & m_{23} & m_{24} \\ m_{31} & m_{32} & m_{33} & m_{34} \\ m_{41} & m_{42} & m_{43} & m_{44} \end{pmatrix} \cdot \begin{pmatrix} I_{real} \\ Q_{real} \\ U_{real} \\ V_{real} \end{pmatrix}$$

$$\begin{aligned} I_{obs} &= m_{11} \cdot I_{real} + m_{12} \cdot Q_{real} + m_{13} \cdot U_{real} + m_{14} \cdot V_{real} \\ Q_{obs} &= m_{21} \cdot I_{real} + m_{22} \cdot Q_{real} + m_{23} \cdot U_{real} + m_{24} \cdot V_{real} \\ U_{obs} &= m_{31} \cdot I_{real} + m_{32} \cdot Q_{real} + m_{33} \cdot U_{real} + m_{34} \cdot V_{real} \\ V_{obs} &= m_{41} \cdot I_{real} + m_{42} \cdot Q_{real} + m_{43} \cdot U_{real} + m_{44} \cdot V_{real} \end{aligned}$$

Method

1. Observe sources with known polarization characteristics
2. Solve the system of equations [1] by fitting our measurements
3. Apply the instrumental polarization correction to our target sources

Full Stokes calibration problems

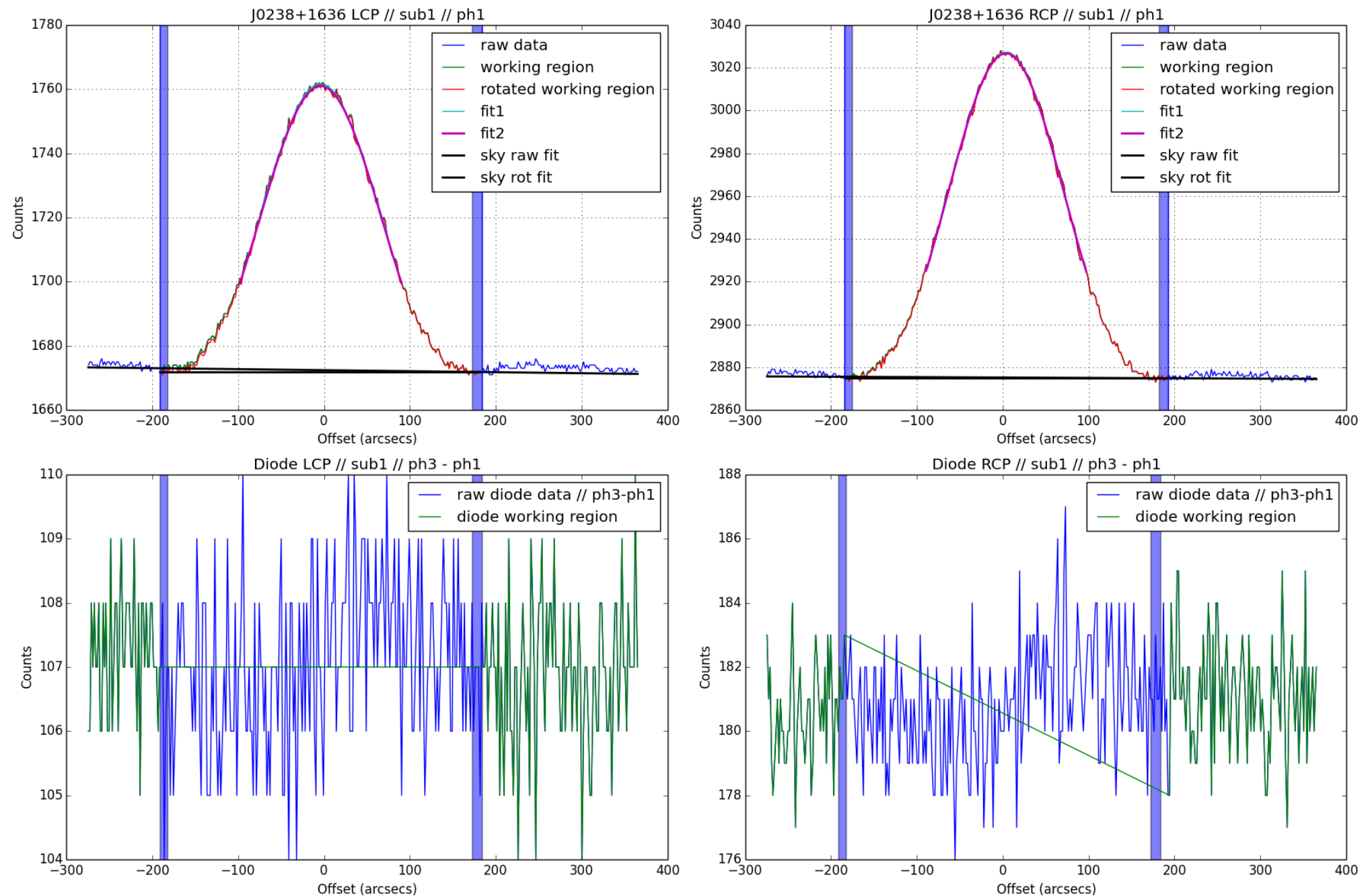
Lack of CP calibrators

Circularly polarized feeds

$$\begin{aligned} I &= |E_l|^2 + |E_r|^2, \\ Q &= 2\text{Re}(E_l^* E_r), \\ U &= -2\text{Im}(E_l^* E_r), \\ V &= |E_l|^2 - |E_r|^2. \end{aligned}$$

Mueller matrix analysis

CP calibration: relative gain (LCP/RCP) correction



Data reduction progress

Since January 2011

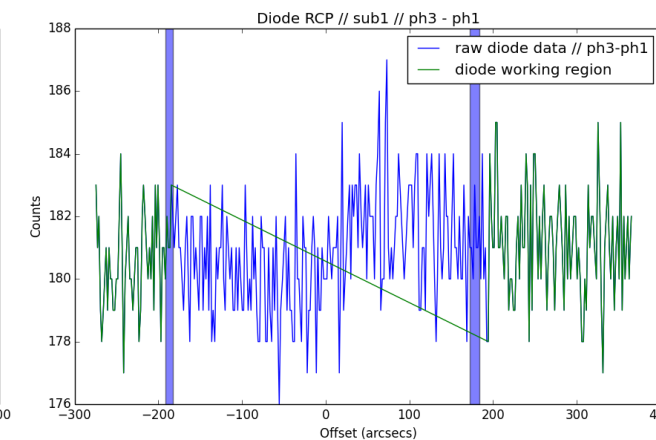
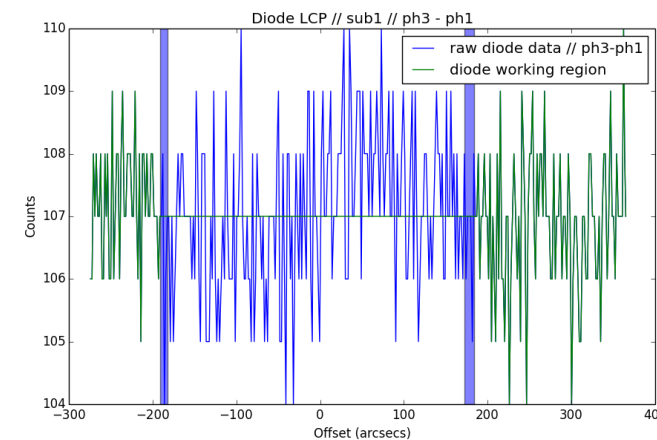
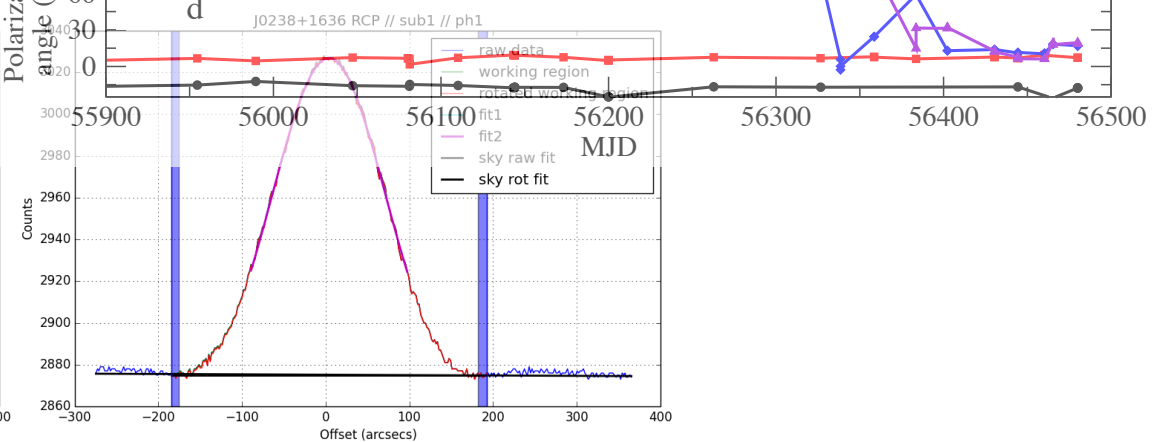
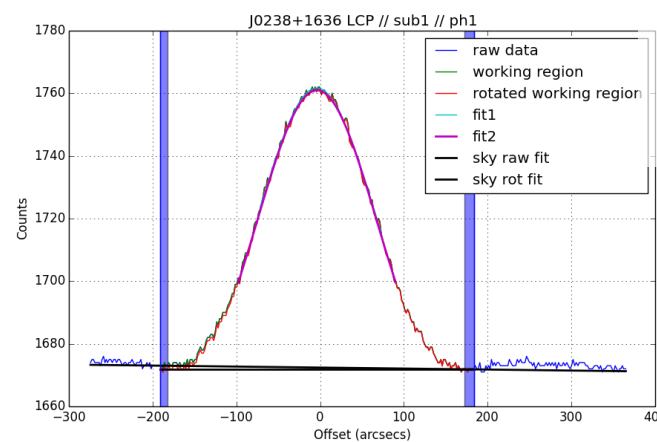
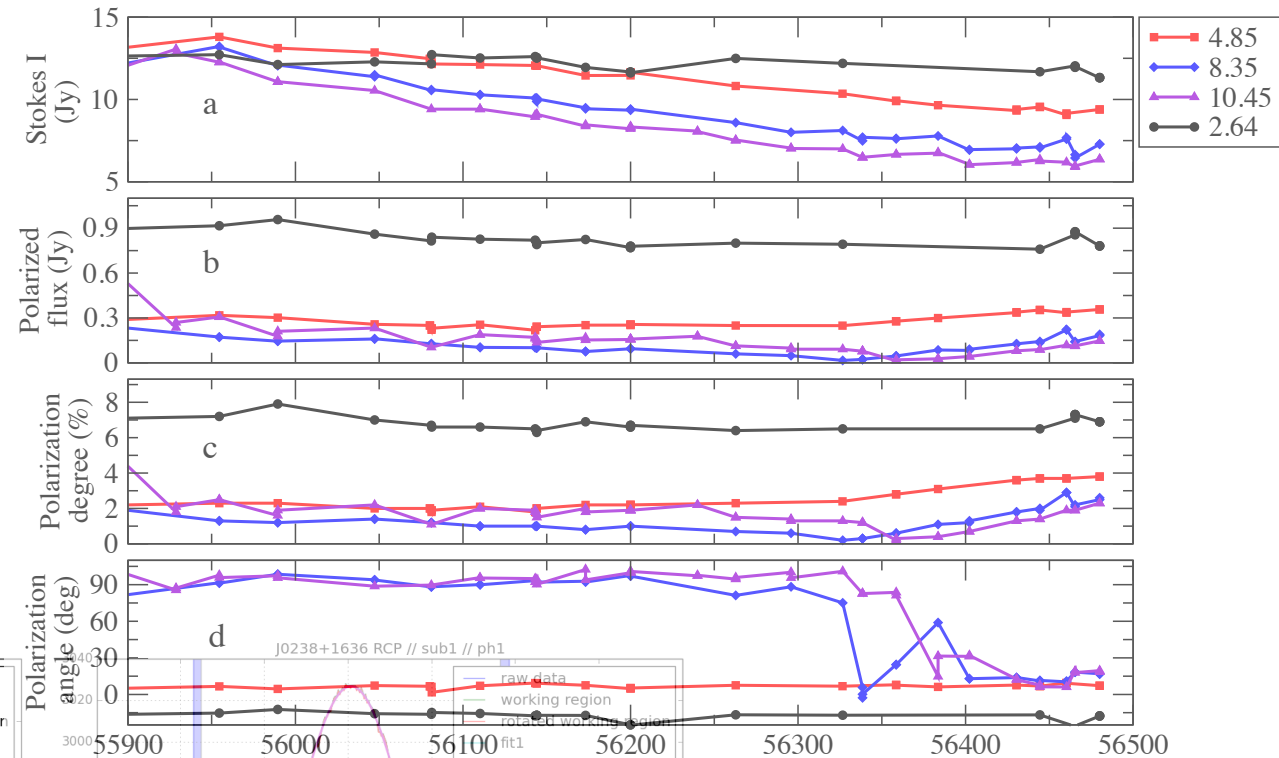
4 frequencies

LP & CP flux

LP & CP degree

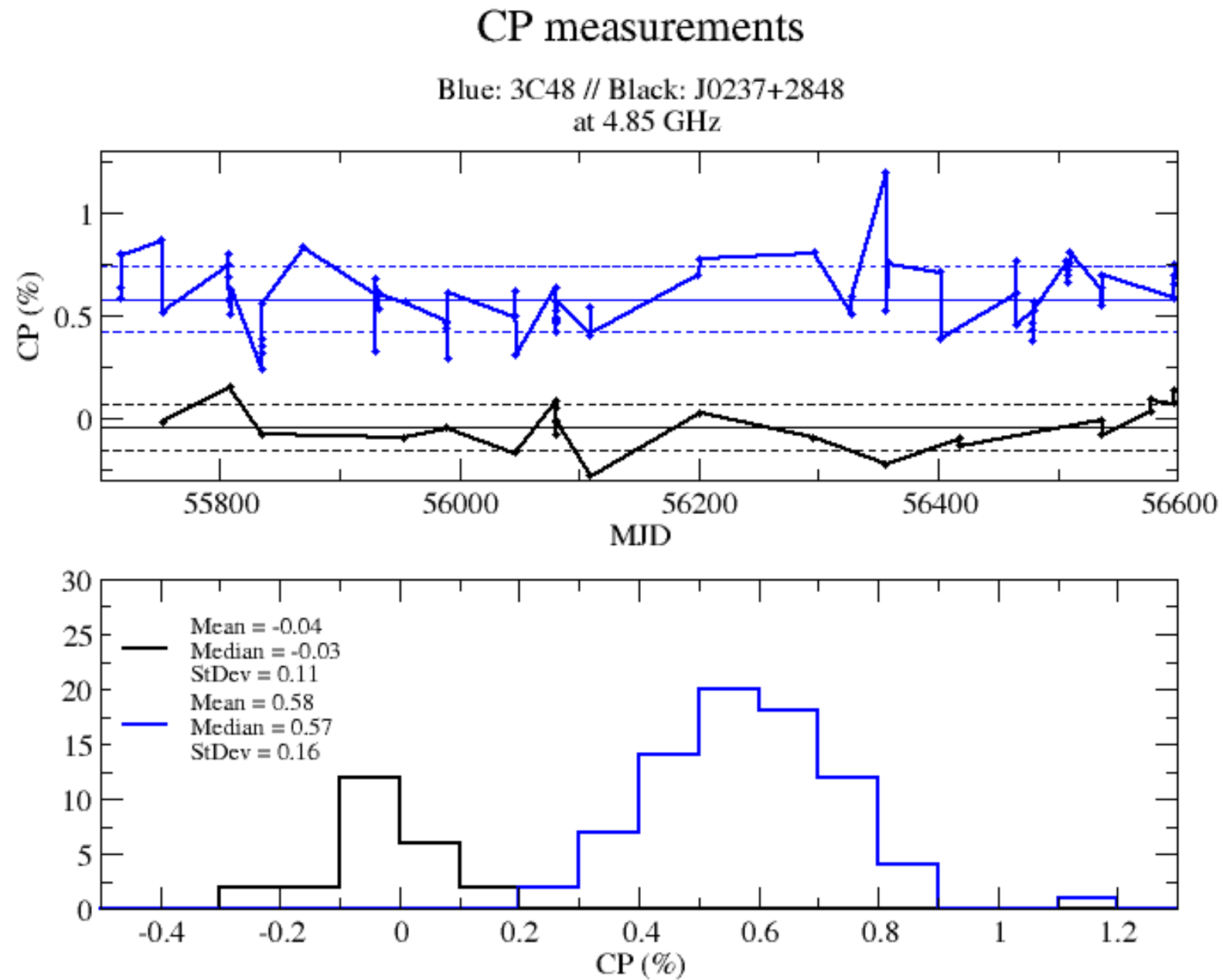
EVPA

3C 454.3
Multiband radio polarization properties



Results

circular polarization calibrator candidates



Results

B-field estimation using CP measurements

Assuming intrinsic CP

$$m_c \sim 100 \left(\frac{\nu_L}{\nu} \right)^{\frac{1}{2}}$$

3C48:

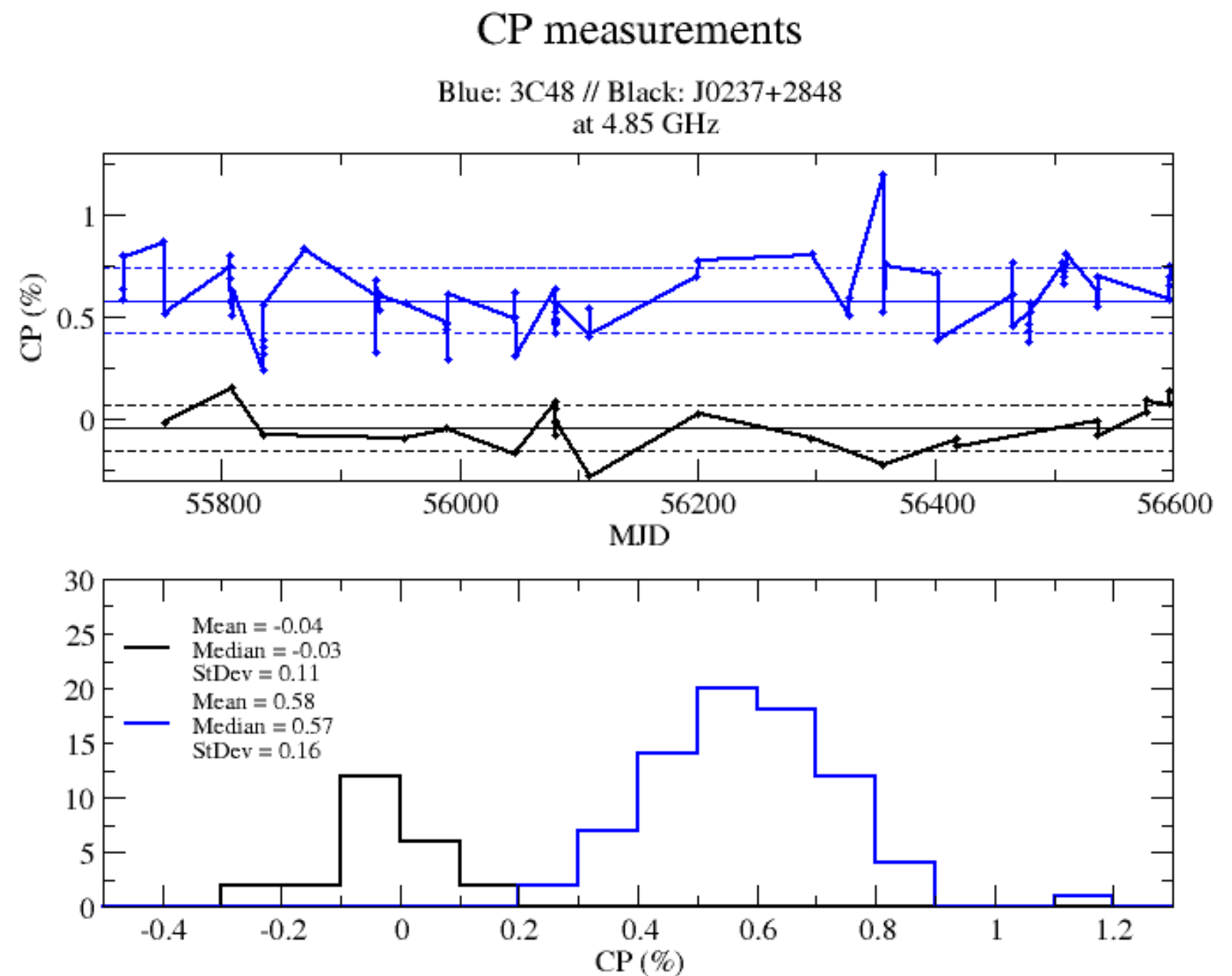
CP = 0.58 %

B = 58mG (electron plasma)

Equipartition:

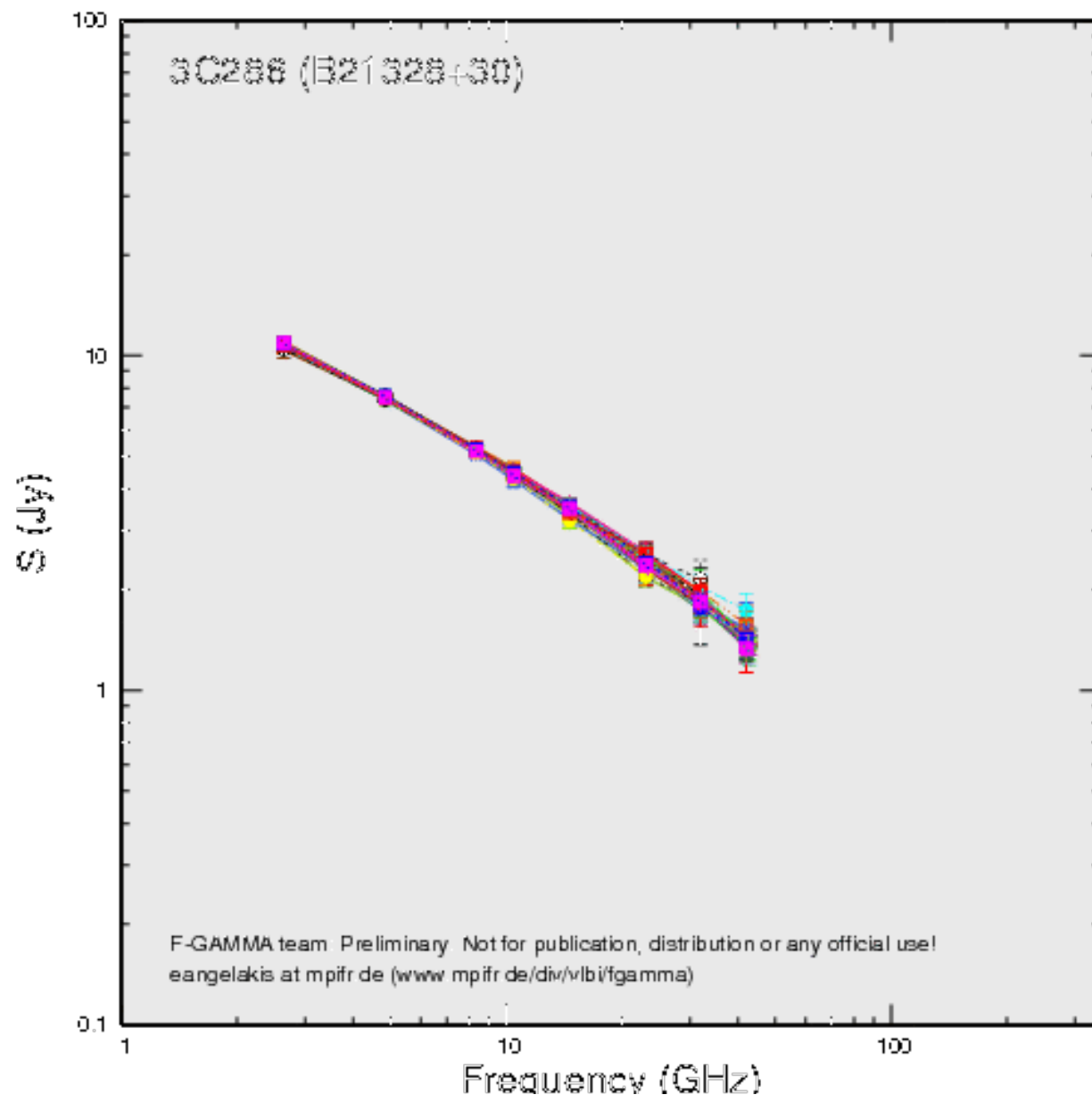
~10 - 100mG

(*O'Sullivan & Gabuzda, 2008*)

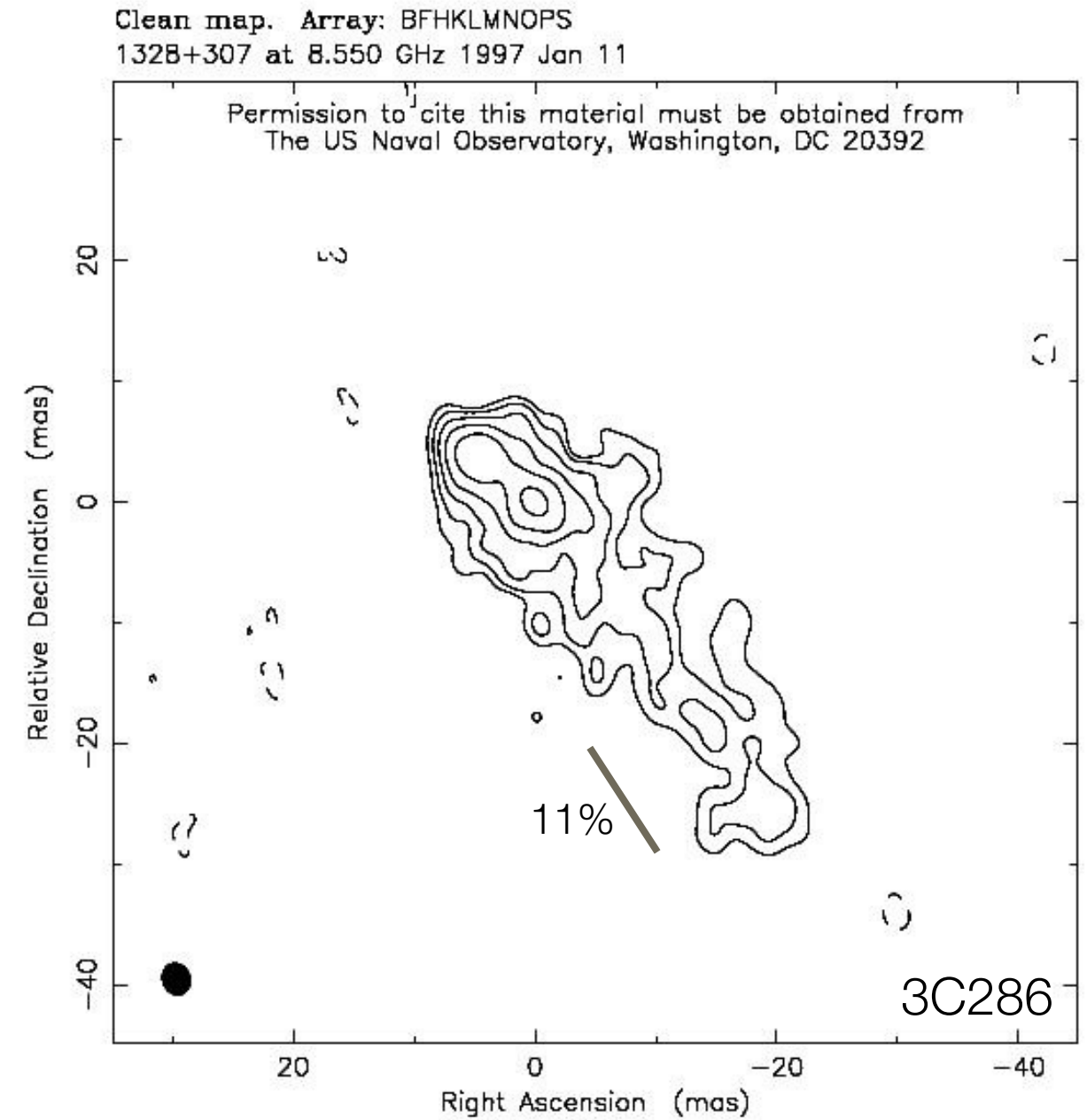


Results

B-field topology

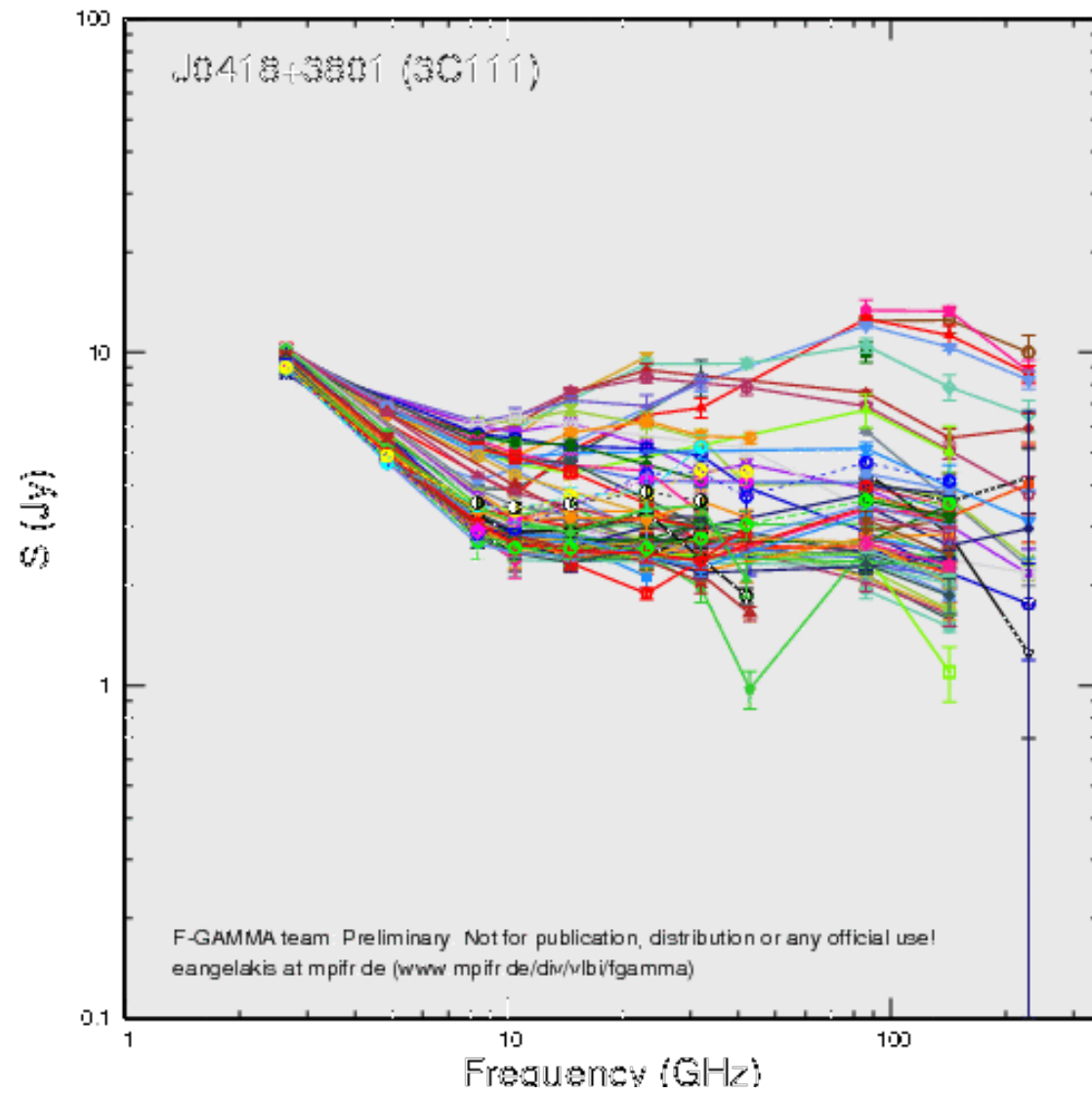


Credit: F-GAMMA team

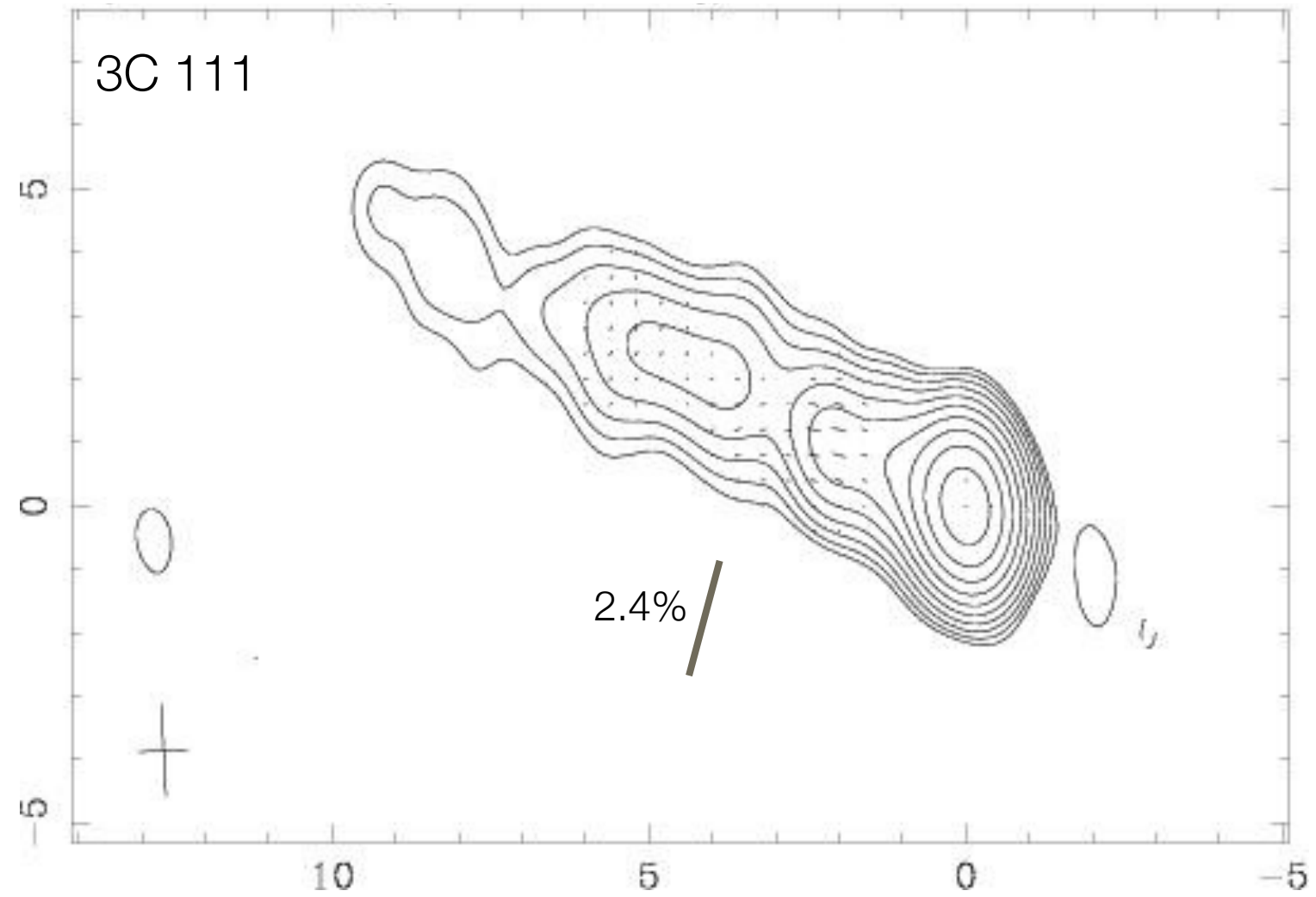


Results

B-field topology

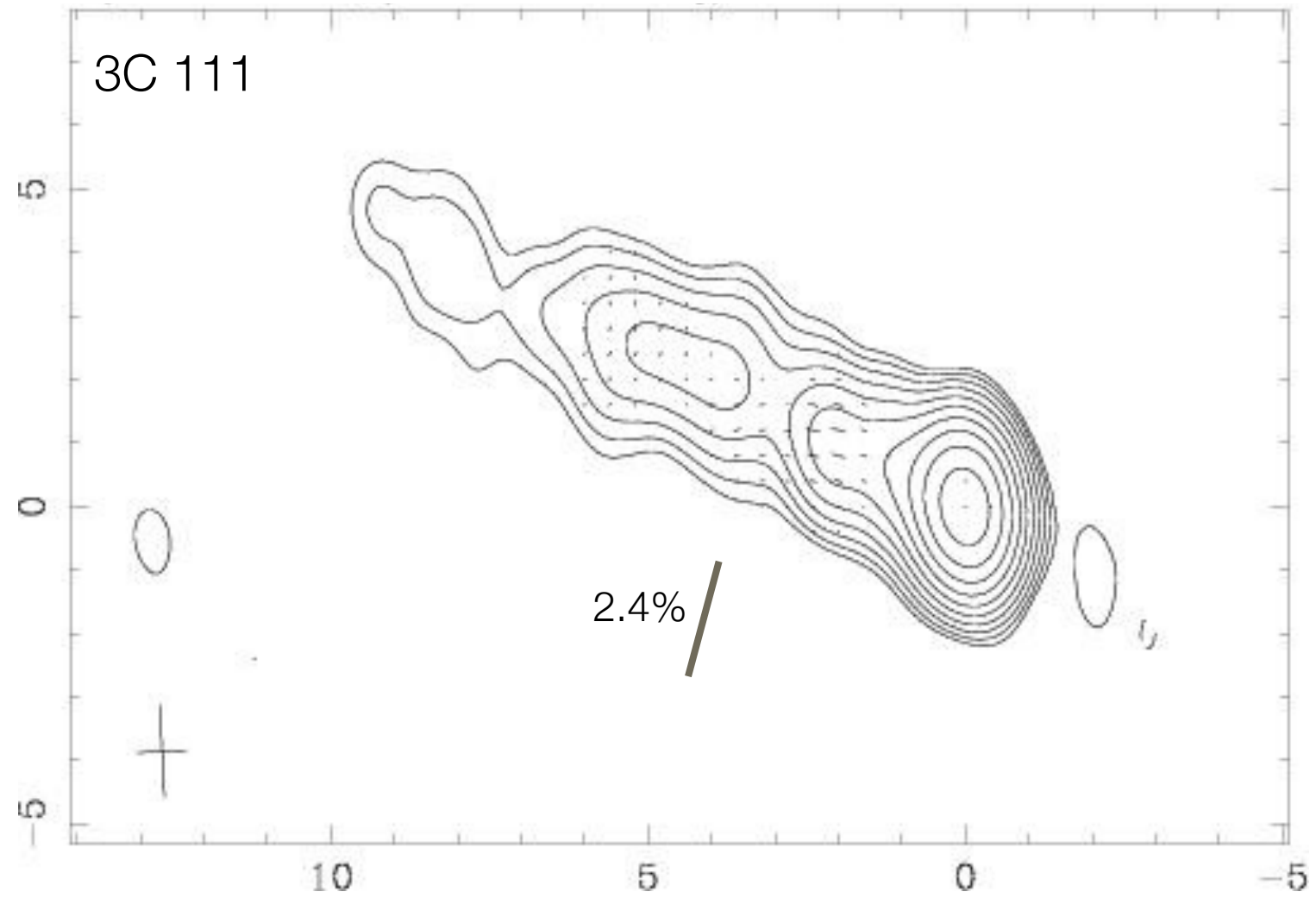
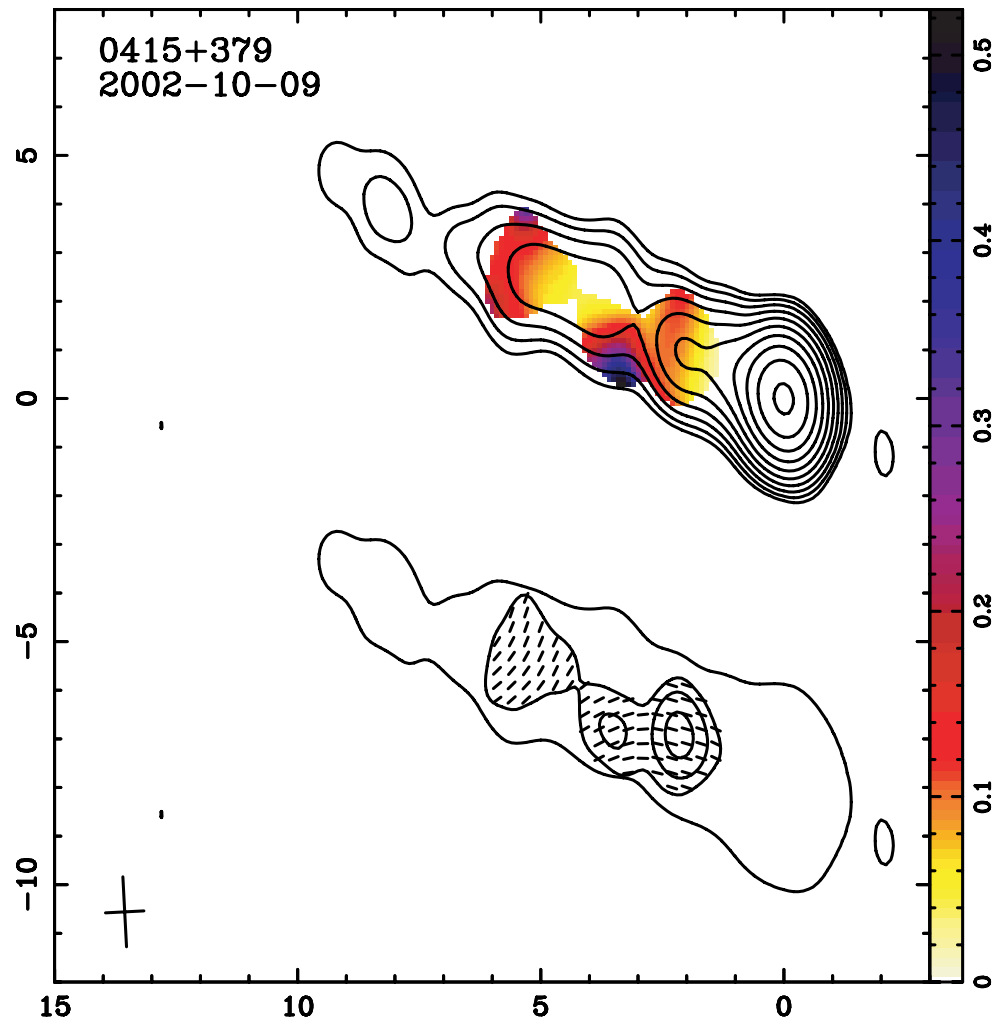


Credit: F-GAMMA team



Results

B-field topology



Credit: MOJAVE team

Results

EVPA swings

PKS 1510-089

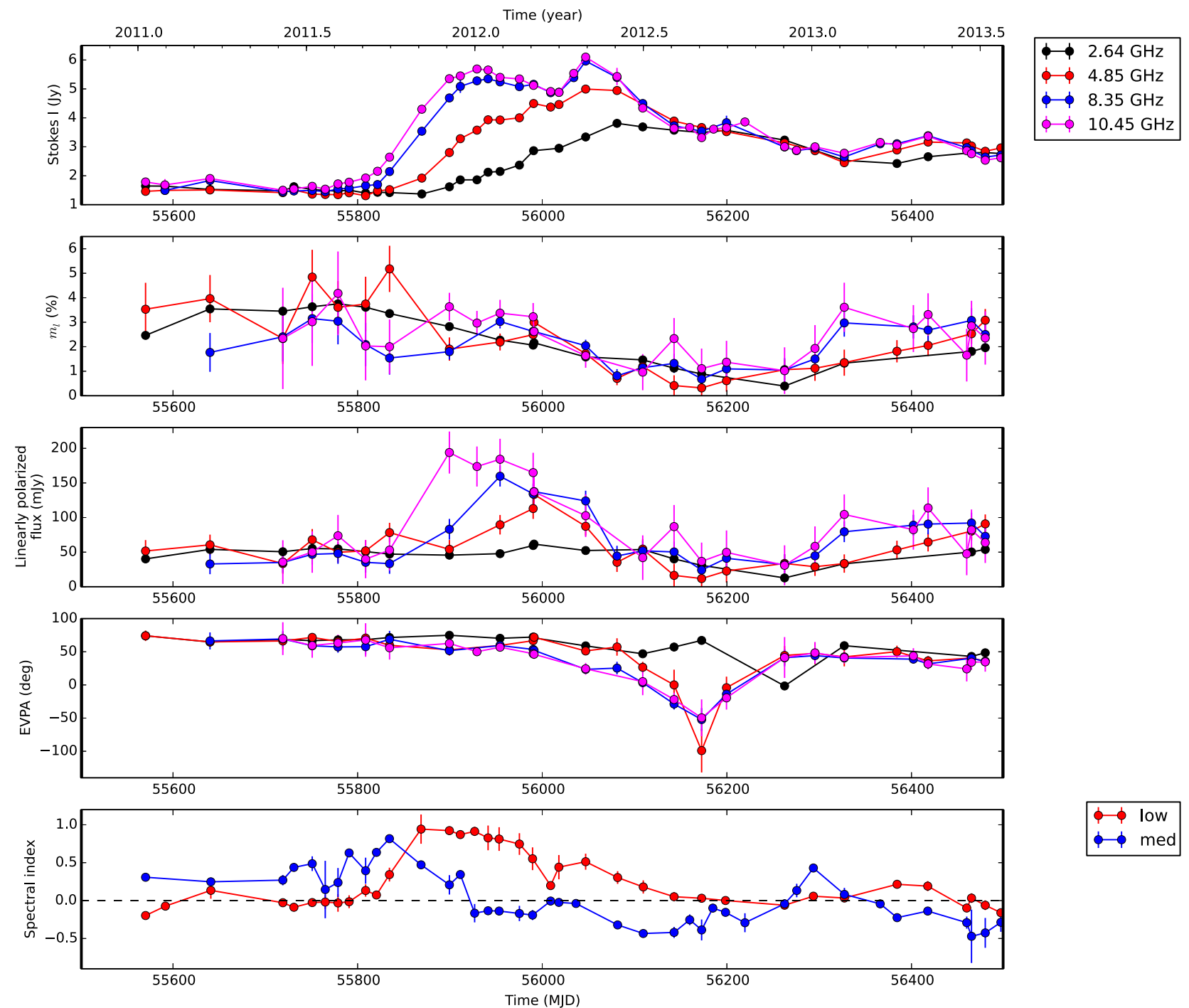
Radiative "swing(s)"

Shows all characteristics of the signature

Multi-band data help the interpretation

CP data are coming...

Difficult to explain with geometrical swing scenario



Results

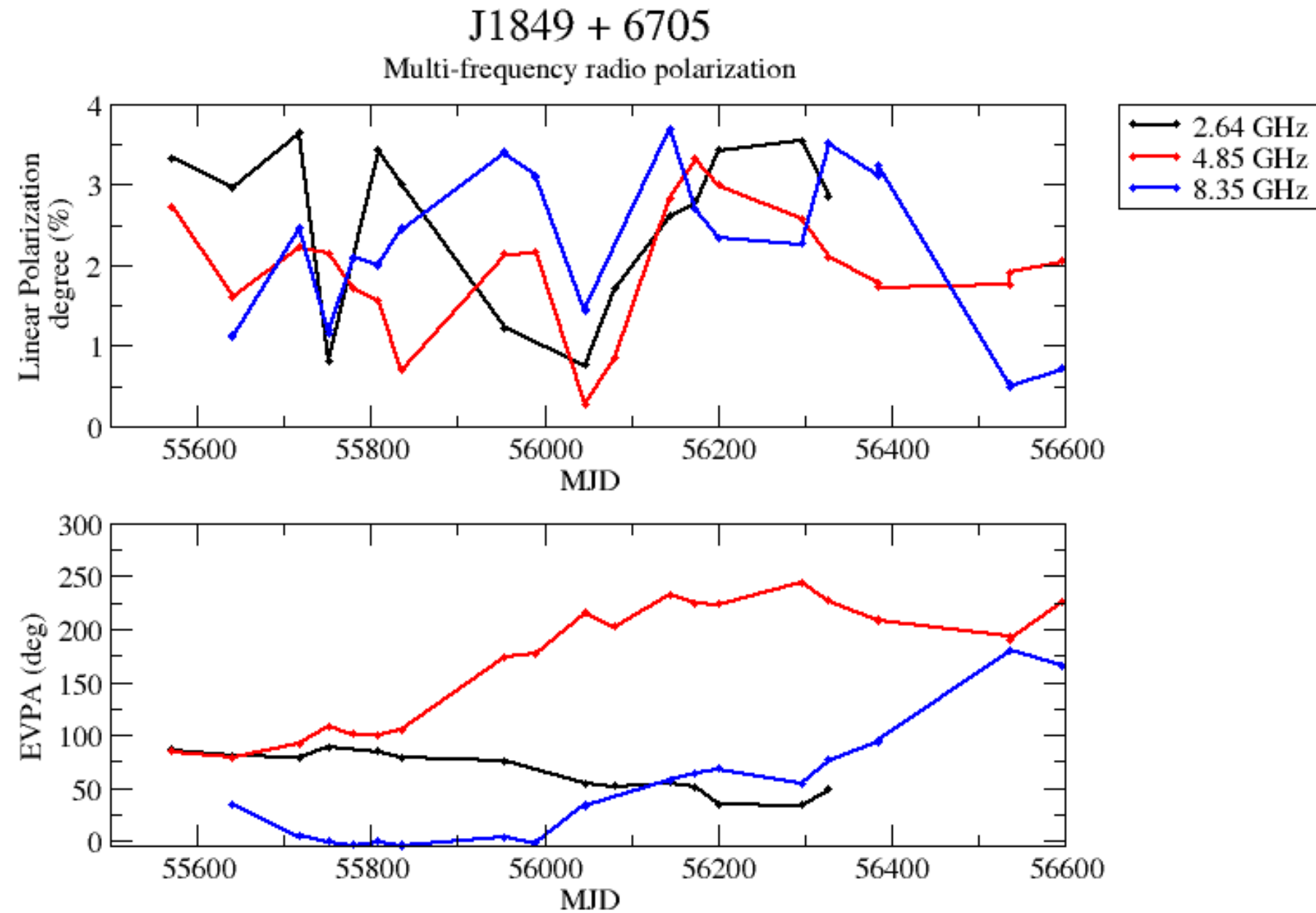
EVPA swings

J1849+6705

Geometrical swing

~175 degrees

Multi-band data help the interpretation



Summary

- Multi-frequency linear and circular radio polarization monitoring data are invaluable for the investigation of the AGN jet physics
- F-GAMMA program
- Data reduction techniques and caveats
- Results